

Field theory of survival probabilities, extreme values, first passage times, and mean span of non-Markovian stochastic processes

Benjamin Walter,^{1,2,3,4} Gunnar Pruessner,^{1,2} and Guillaume Salbreux^{5,6}

¹*Department of Mathematics, Imperial College London,
180 Queen's Gate, SW7 2AZ London, United Kingdom*

²*Centre for Complexity & Networks, Imperial College London, SW7 2AZ London, United Kingdom*

³*SISSA-International School for Advanced Studies, via Bonomea 265, 34136 Trieste, Italy*

⁴*INFN, Sezione di Trieste, 34136 Trieste, Italy**

⁵*The Francis Crick Institute, 1 Midland Road, NW1 1AT London, United Kingdom*

⁶*Department of Genetics and Evolution, University of Geneva,
Quai Ernest-Ansermet 30, 1205 Geneva, Switzerland*

(Dated: September 9, 2021)

We provide a perturbative framework to calculate extreme events of non-Markovian processes, by mapping the stochastic process to a two-species reaction diffusion process in a Doi-Peliti field theory combined with the Martin-Siggia-Rose formalism. This field theory treats interactions and the effect of external, possibly self-correlated noise in a perturbation about a Markovian process, thereby providing a systematic, diagrammatic approach to extreme events. We apply the formalism to Brownian Motion and calculate its survival probability distribution subject to self-correlated noise.

Introduction— Many non-equilibrium systems are studied by projecting out a single slow degree of freedom which evolves stochastically and often displays non-negligible memory effects [1–3]. A classic object of study is its survival probability which describes the probability of the degree of freedom not having reached a threshold yet [4, 5]. The survival probability defines not only the persistence exponents [6], but is also closely linked to the distribution of first-passage times, running maxima, and spans via some simple relations. All of these *extreme events* aptly characterise the non-equilibrium nature of complex systems and have been studied separately over the last hundred years (for classic references see [7–11], for recent overviews [12, 13]). Survival probabilities of non-Markovian processes are, however, notoriously hard to compute as they depend on the entire trajectory whose distribution is usually impossible to obtain. Perturbative schemes such as [14, 15] have proven to be successful in characterising the behaviour of the survival probabilities for large times in classical non-equilibrium models. More recently, a similar perturbation theory has been applied to fractional Brownian Motion to further access the full survival probability in a perturbation theory about the Hurst parameter [16, 17]. These techniques, however, heavily rely on Gaussianity and do not readily translate to more general non-Gaussian non-Markovian processes. In this letter, we compute the *full* survival probability of processes subject to both uncorrelated and self-correlated noise in a perturbation theory in the strength of the self-correlated noise. This type of process is central to the study of active matter [18–22] and more generally non-equilibrium phenomena [23–25].

In our recent work [26], we presented a scheme to calculate first-passage distributions for the same class of

non-Markovian processes. These results relied on a perturbative functional expansion of a renewal type equation inspired by the classical work of [10, 27]. Using a field-theoretic approach that draws on both the Doi-Peliti [28, 29] as well as the Martin-Siggia-Rose formalism [30], in the present work we generalise these results to a broader class of extreme events.

Using a field theory has some notable advantages. Firstly, the diagrammatics give a clear intuition of the underlying microscopic processes otherwise hidden within cumbersome expressions. Secondly, the field theory provides a systematic perturbative framework naturally drawing on renormalisation techniques. Thirdly, it is easily extended to incorporate further interactions, such as reactions, external and pair potentials.

This letter is structured as follows. First, we map a Markovian process onto a field theory. Secondly, we introduce a field-theoretic mechanism which is designed to keep track of the space already visited by the process. This defines the visit probability $\mathcal{Q}(x_0, x_1, t)$, the probability that the process started at x_0 has been at x_1 prior to time t , and which is the complement of the survival probability. Thirdly, we add the self-correlated driving noise, thus breaking Markovianity, and compute the corrections induced in \mathcal{Q} . Finally, we illustrate the approach by computing the correction to the survival probability of Brownian Motion driven by self-correlated noise.

Field theory for Markovian visit probabilities— In this letter, we study stochastic processes characterised by a Langevin Equation [31],

$$\begin{aligned} \dot{x}_t &= -V'(x_t) + \xi_t \\ x(t = t_0) &= x_0 \end{aligned} \quad (1)$$

where $V'(x_t)$ is the gradient of a potential and ξ_t Gaussian white noise with correlator $\langle \xi_t \xi_{t'} \rangle = 2D_x \delta(t - t')$. Further, we introduce $T(x, t) \equiv T(x_0, x; t_0, t)$ as the *transition probability* for the walker to travel from x_0 at time

* bwalter@sissa.it

t_0 to x at time t . We will state x_0 and t_0 only where needed for clarity. As is detailed in [32], the process (1) can be mapped to a Doi-Peliti field theory [32–34] containing two fields, the annihilator field $\varphi(x, t)$ and the creator field $\varphi^\dagger(x, t) = 1 + \tilde{\varphi}(x, t)$, which are jointly distributed according to

$$\mathcal{P}[\varphi, \tilde{\varphi}] = \exp(-\mathcal{S}_\varphi[\varphi, \tilde{\varphi}]) . \quad (2)$$

where the action $\mathcal{S}_\varphi[\varphi, \tilde{\varphi}]$ is constructed as

$$\mathcal{S}_\varphi = \iint dx dt \tilde{\varphi} (\partial_t - V''(x) - V'(x)\partial_x - D\partial_x^2) \varphi . \quad (3)$$

Moreover, the transition probability satisfies

$$T(x, t) = \langle \varphi(x, t)(1 + \tilde{\varphi}(x_0, t_0)) \rangle_{\mathcal{S}_\varphi} , \quad (4)$$

where $\langle \bullet \rangle_{\mathcal{S}_\varphi}$ denotes the expectation over the measure (2).

The key problem we address in this letter is how to approximate the distribution of first-passage times, running maxima, and mean volume explored of the process defined in Eq. (1). These *extreme events* are all mutually related via the *visit probability* which we define as $\mathcal{Q}(x_0, x, t_0, t) = \mathcal{Q}(x, t) = \mathbb{P}[x_s = x \text{ at some time } t_0 \leq s \leq t]$, i.e. the complement of the *survival probability* $\mathbb{P}_{\text{surv}} = 1 - \mathcal{Q}$. This density measures the probability that the particle has been at x at or before time t . The visit probability contains various informations about the process: When taking the derivative $\partial_t \mathcal{Q}(x, t)$, one measures the weight of those paths which visit x at t for the first time. The latter is the first-passage time, and thus its distribution satisfies

$$\mathbb{P}_{\text{FPT}}(\tau_{x_0, x_1} = t) = \partial_t \mathcal{Q}(x_1, t) . \quad (5)$$

Analogously, taking the derivative $-\partial_x \mathcal{Q}(x, t)$, weighs those paths who at time t visit x_1 for the first time, or alternatively, the distribution of the maximum $\hat{x}_t = \max_{s \leq t} x_s$, i.e.

$$\mathbb{P}_{\text{Max}}(\hat{x}_t = x) = -\partial_x \mathcal{Q}(x, t) . \quad (6)$$

Moreover, integrating over $\int dx \mathcal{Q}(x, t)$, gives the average of the volume explored, which is defined as the difference between running maximum and minimum, $\text{Vol}([x_t], t) = \max_{s \leq t} x_s - \min_{s \leq t} x_s$. Its mean is given by

$$\langle \text{Vol} \rangle = \int dx \mathcal{Q}(x, t) . \quad (7)$$

Higher moments of the span are considered in [35].

As is explained in great detail in [35–37], and briefly discussed in App. A, the visit probability $\mathcal{Q}(x, t)$ can be expressed as a field-theoretic expectation value under a Doi-Peliti field theory by introducing two additional auxiliary (“trace”-) fields $\psi(x, t)$ and $\tilde{\psi}(x, t)$ with a joint distribution

$$\begin{aligned} \mathcal{P}[\varphi, \tilde{\varphi}, \psi, \tilde{\psi}] \\ = \lim_{\gamma \uparrow \infty} \exp \left(-\mathcal{S}_\varphi[\varphi, \tilde{\varphi}] - \mathcal{S}_\psi[\psi, \tilde{\psi}] + \gamma \mathcal{S}_\gamma[\varphi, \tilde{\varphi}, \psi, \tilde{\psi}] \right) \end{aligned} \quad (8)$$

such that the visit probability can be written as

$$\mathcal{Q}(x, t) = \lim_{\gamma \uparrow \infty} \langle \psi(x, t) (1 + \tilde{\varphi}(x_0, t_0)) \rangle_{\mathcal{S}} \quad (9)$$

where $\langle \bullet \rangle_{\mathcal{S}}$ is understood as the average with respect to the measure in Eq. (8). Here, \mathcal{S}_ψ denotes the *trace action*

$$\mathcal{S}_\psi = \iint dx dt \tilde{\psi} (\partial_t + \varepsilon) \psi , \quad (10)$$

describing a field with vanishing mass $\varepsilon > 0$ which regularises the infrared, ensures causality [35, 38], and is to be taken to $\varepsilon \rightarrow 0^+$ at the end of any calculation.

The *deposition action* is derived in [36] and reads

$$\mathcal{S}_\gamma = \iint dx dt \left(\tau \tilde{\psi} \varphi + \sigma \tilde{\varphi} \tilde{\psi} \varphi - \lambda \tilde{\psi} \varphi \psi - \kappa \tilde{\varphi} \tilde{\psi} \varphi \psi \right) \quad (11)$$

where we only included infrared-relevant vertices. The four dimensionfull couplings τ, σ, κ and λ , are introduced as differently for independent renormalisation. However, the rates τ and σ and the densities κ, λ are each equal at bare level and are related to each other via $\lambda = \kappa = n_0 \tau = n_0 \sigma$ where n_0 is the so-called carrying-capacity (see App. A for details). Overall, \mathcal{S}_γ is multiplied with a dimensionless constant γ which needs to be taken to $\gamma \uparrow \infty$.

Each of the four vertices in (11) is diagrammatically represented as

$$\begin{array}{cccc} \tau & \sigma & -\lambda & -\kappa \\ \text{---} & \text{---} & \text{---} & \text{---} \\ \text{wavy} & \text{wavy} & \text{wavy} & \text{wavy} \end{array} \quad (12)$$

and enters into the action multiplied by γ . Here, straight red lines represent the propagators of $\varphi, \tilde{\varphi}$, and green wiggly lines those of $\tilde{\psi}, \psi$. As a convention, we read vertices/diagrams from right to left.

It follows that the diagrammatic expansion of the trace function (9) is

$$\mathcal{Q}(x, t) = n_0^{-1} \lim_{\gamma \uparrow \infty} \begin{array}{c} (x, t) \\ \text{---} \\ \text{wavy} \bullet \text{---} \\ (x_0, t_0) \end{array} \quad (13)$$

where the central dot stands for the renormalised coupling τ_R . This renormalisation is given by the diagrammatic expansion

$$\begin{aligned} \tau_R &= \text{---} \bullet \text{---} \\ &= \gamma \text{---} + \gamma^2 \text{---} + \gamma^3 \text{---} + \dots \end{aligned} \quad (14)$$

The only diagrams contributing to this expansions are chains of the loop-diagram . As shown in App. B the fully renormalised vertex can be evaluated using a geometric or Dyson sum as

$$\tau_R(\omega) = \frac{\gamma \tau}{1 + \gamma \kappa R(x_1, \omega)} \quad (15)$$

which is an *exact* result for all γ , such that the effective trace function, Fourier transformed, is

$$\int dt e^{i\omega t} \mathcal{Q}(x, t) = \lim_{\gamma \rightarrow \infty} \frac{1}{-i\omega + \varepsilon} \tau_R(\omega) T(x_0, x_1, \omega) = \frac{1}{-i\omega} \frac{T(x_0, x_1, \omega)}{R(x_1, \omega)} \quad (16)$$

where we made use of time-translational invariance to write the Fourier-transform in one frequency only, tacitly took the limit $\varepsilon \rightarrow 0$, and used $n_0\tau = \kappa$. Multiplying this result with $(-i\omega)$ gives the first-passage time moment generating function. Then, the result in (16) agrees with classical results given in [10, 27].

Non-Markovian visit probabilities: A perturbative approach—Stochastic processes are Markovian if and only if their driving noise is δ -correlated [39]. As a perturbative generalisation to non-Markovian processes, we thus extend the class of processes given by (1) to

$$\dot{x}_t = -V'(x_t) + \xi_t + gy_t \quad (17)$$

The additional driving noise y_t is assumed to be stationary with zero mean and a general autocorrelation function

$$C_2(t-s) = \overline{y_s y_t}. \quad (18)$$

By $\overline{\bullet}$ we denote in the following averages over the path distribution of y_t . Importantly, y is not required to be Gaussian such that higher non-trivial cumulants $C_n(t_2 - t_1, \dots, t_n - t_{n-1}) = \langle y_{t_1} \dots y_{t_n} \rangle_c$ may exist, but enter only at perturbative order g^n . The dimensionless coupling constant g is assumed to be small ($g \ll 1$). To fixed order in g and for suitable choice of y_t , processes of the type Eq. (17) can be both short-ranged such as for run-and-tumble particles in noisy environments [18, 20] or long-ranged, such as processes driven by fractional Gaussian noise [19], as long as $C_2(t)$ is integrable in a sense made rigorous later (cf. Eq. (25)). In what follows, we derive the visit probability $\overline{\mathcal{Q}(x, t)}$ averaged over both, the Gaussian white noise ξ_t and the driving noise y_t to first leading perturbative order g^2 .

As is outlined in the App. C, the visit probability conditioned on a *fixed realisation* of the driving noise can still be obtained by Eq. (9) using the average with respect to the modified path measure

$$\begin{aligned} & \overline{\mathcal{P}[\varphi, \tilde{\varphi}, \psi, \tilde{\psi}]} \\ &= \lim_{\gamma \rightarrow \infty} \int \mathcal{D}[y_t] \exp \left(-\mathcal{S}_\varphi[\varphi, \tilde{\varphi}] - \mathcal{S}_\psi[\psi, \tilde{\psi}] \right. \\ & \quad \left. + \gamma \mathcal{S}_\gamma[\varphi, \tilde{\varphi}, \psi, \tilde{\psi}] + \iint gy_t \tilde{\varphi} \partial_x \varphi \right) \mathcal{P}[y_t], \quad (19) \end{aligned}$$

As is shown in the App. C, one can compute averages with respect to this y_t -dependent path-average, to then

integrate over the path measure of y_t . As it turns out, one does not need to know the full path measure of y_t , but can instead rewrite the double average $\overline{\langle \bullet \rangle}$ using the *moment generating functional* of y_t which is defined as

$$\mathcal{Z}_y[g \cdot j_t] = \int \mathcal{D}[y_t] e^{g \int dt j_t y_t} \mathcal{P}[y_t]. \quad (20)$$

Expanding the exponential to second order, and averaging over y_t , gives (cf. Eq. (18))

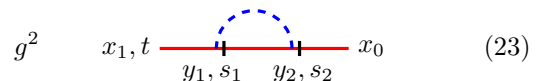
$$\mathcal{Z}_y[g \cdot j_t] = 1 + \frac{1}{2} g^2 \iint dt_1 dt_2 j_{t_1} C_2(t_2 - t_1) j_{t_2} + \mathcal{O}(g^3). \quad (21)$$

Therefore, we may approximate expectation values such as the one appearing in Eq. (19) using the identity

$$\overline{\langle \bullet \rangle_S} = \left\langle \bullet \cdot \mathcal{Z}_y \left[g \iint dx dt \tilde{\varphi} \partial_x \varphi \right] \right\rangle_S. \quad (22)$$

which to this perturbative order only contains $C_2(t-s)$, the correlation function of y_t (Eq. (18)).

Diagrammatically speaking, this amounts to computing the same diagrams as in Eq. (14), but additionally decorating them with driving noise correlation loops represented as



$$g^2 \quad x_1, t \text{ --- } y_1, s_1 \text{ --- } y_2, s_2 \text{ --- } x_0 \quad (23)$$

As in Eq. (12), red solid lines denote bare transition probabilities. The blue dashed line connecting two internal vertices, (cf. Eq. (21) and App. C), represents the correlation kernel $C_2(s_2, s_1)$. The two vertical bars inserted to the right of each such vertex represent the gradient operator acting on the target point of the incoming transition probability. Combinatorially, there are four ways in which these loops decorate the diagrams of the (Markovian) visit probability, which are displayed in Fig. 1. As is shown in the App. E, the new visit probability, $\mathcal{Q}(x, t) = \langle \psi(x, t) \tilde{\varphi}(0, 0) \mathcal{Z}_y[g \int \tilde{\varphi} \nabla \varphi] \rangle_S$, acquires a functionally similar form to the Markovian case (16)

$$\begin{aligned} & \mathcal{Q}(x_0, x_1, t) \\ &= \int d\omega \frac{e^{-i\omega t}}{-i\omega} \frac{T^{(0)}(x_0, x_1, \omega) + g^2 T^{(2)}(x_0, x_1, \omega)}{R^{(0)}(x_1, \omega) + g^2 R^{(2)}(x_1, \omega)} + \mathcal{O}(g^3) \quad (24) \end{aligned}$$

Here, as we do from now on, we denote the (Fourier transformed) Markovian transition probability density of the undriven process in Eq. (1) as $T^{(0)}(x_0, x_1, \omega)$ instead of $T(x_0, x_1, \omega)$, and analogously, $R^{(0)}(x_1, \omega) = T^{(0)}(x_1, x_1, \omega)$. Further, we introduced the g^2 correction to the y_t -averaged transition probability

$$T^{(2)}(x_0, x_1, \omega) = \iint dy_1 dy_2 d\tilde{\omega} \left[\frac{T^{(0)}(y_1, x_1, \omega - \tilde{\omega})}{R^{(0)}(x_1, \omega - \tilde{\omega})} T^{(0)}(x_1, y_2, \omega - \tilde{\omega}) - T^{(0)}(y_1, y_2, \omega - \tilde{\omega}) \right] \times \left(\partial_{y_1} T^{(0)}(x_0, y_1, \omega) \right) \left(\partial_{y_2} T^{(0)}(y_2, x_1, \omega) \right) \hat{C}_2(\tilde{\omega}). \quad (25)$$

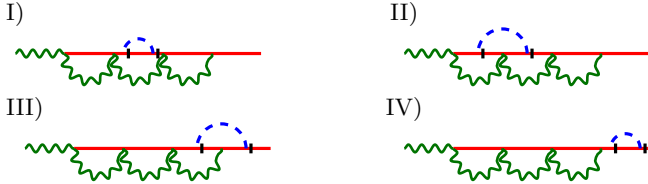


Figure 1. Diagrammatic representation of the four different kinds of terms appearing in the perturbative expansion of \mathcal{Q} (cf. Eq. (C12) and (23)). The Markovian diagrams (cf. Eq. (14)) are corrected by the external driving noise $g \cdot y_t$, giving rise to the expansion Eq. (C12). These four types of diagrams result in four different correction terms explicitly derived in App. E, and which together give the final result for the driving noise corrected transition probability stated in Eq. (25).

and, analogously, $R^{(2)}(x_1, \omega) = T^{(2)}(x_1, x_1, \omega)$.

In the case of a Brownian Motion additionally driven by self-correlated noise, the second order corrections given by Eq. (25) drastically simplifies as shall be demonstrated below.

Example: Brownian Motion driven by self-correlated noise— We briefly discuss the example process of active thermal Brownian motion (ATBM, [26]) on a real line. In our previous article [26], we found the perturbative correction to the first-passage time moment generating function for an active thermal Ornstein Uhlenbeck process, and an active Brownian Motion on a ring. Since the distribution of first-passage times and visits are closely linked via $\mathcal{Q}(x, \omega) = (-i\omega)^{-1} \chi_{\text{FPT}}(x, \omega)$, we report the visit probabilities of the latter two processes in App. G.

To illustrate the method outlined above we use the example of ATBM on a real line defined via

$$\dot{x}_t = \xi_t + g y_t \quad (26)$$

where ξ_t is white noise of strength $\langle \xi_s \xi_t \rangle = 2D_x \delta(t - s)$, and y_t is a stationary, not necessarily Gaussian, driving noise with a non-white self-correlation function $C_2(|s - t|) = \langle y_s y_t \rangle$. Without loss of generality, we assume $x_0 = 0$ and $x_1 > 0$. The transition probability $T(x_0, x_1, \omega) = T(x = x_1 - x_0, \omega)$ of simple Brownian motion, $g = 0$, is given by $T^{(0)}(x, t) = (4\pi D_x t)^{-1/2} \exp\left(-\frac{x^2}{4D_x t}\right)$, so

that $T^{(0)}(x, \omega) = (\sqrt{-4i\omega D_x})^{-1} \exp(-\sqrt{-i\omega/D_x}|x|)$ and $\mathcal{Q}(x, t) = 1 - \text{erf}((4D_x t)^{-1/2}|x|)$ via Eq. (16) and a subsequent inverse Fourier transform.

For $g \neq 0$, we compute the correction $T^{(2)}(x, \omega)$ using Eq. (25). As is detailed in App. F, the integral simplifies drastically, and we state here only the results, which can be summarised most succinctly using a “time-stretch function” $\Upsilon(t)$ as follows. Given the correlation function $C_2(t)$, Eq. (18), it is defined as

$$\Upsilon(t) = \int_0^t ds s C_2(t - s) = \int_0^t du \int_0^u ds C_2(s), \quad (27)$$

or, alternatively, $\partial_t^2 \Upsilon(t) = C_2(t)$. The second order correction to the transition probability can then be written as

$$T^{(2)}(x_0, x_1, \omega) = \int dt e^{-i\omega t} \Upsilon(t) (\partial_{x_1}^2) T^{(0)}(x_0, x_1, t) = \int dt e^{-i\omega t} D_x^{-1} \Upsilon(t) \partial_t T^{(0)}(x_0, x_1, t) \quad (28)$$

where we made use of the Brownian relation $\partial_t T^{(0)}(x, t) = D_x \partial_x^2 T^{(0)}(x, t)$. In real time, the correction $T^{(2)}(x_0, x_1, t) = D_x^{-1} \Upsilon(t) \partial_t T^{(0)}(x, t)$ can be absorbed into the t -dependence of the tree-level as

$$T(x, t) = T^{(0)}(x, t + g^2 D_x^{-1} \Upsilon(t)) + \mathcal{O}(g^3). \quad (29)$$

The externally driven non-Markovian process x_t has therefore transition probabilities that are, to order g^2 , equal to those of a time-stretched Brownian motion with $t \mapsto \tau(t) = (1 + g^2 (D_x t)^{-1} \Upsilon(t)) t$, thus $x_t \stackrel{d}{=} \sqrt{2D_x} W_{\tau(t)}$. That, however, does not mean that the return probabilities agree between the original, externally driven non-Markovian process x_t and the time-stretched Brownian motion, because of the latter not accounting for the now hidden variable y_t . The time-stretched Brownian motion ignores correlations between that y_t and x_t . For example, the transition probability is no longer correctly given by the first passage and repeated return, as first passage is favoured for particular values of y_t that the subsequent return does not account for.

Returning to Eq. (24), and using Eq. (28), we slightly rephrase the result for driven Brownian Motion by explicitly expanding in g^2 to

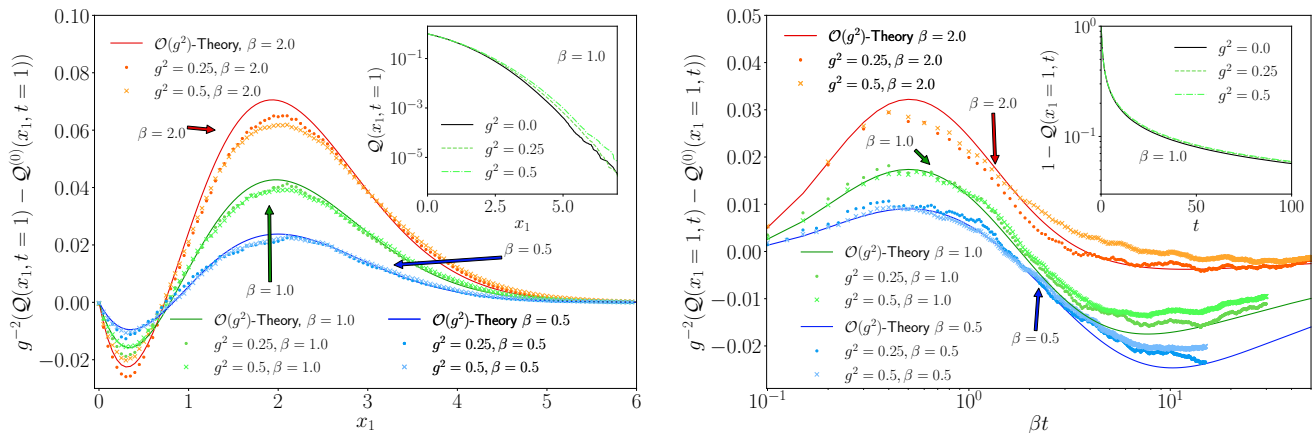


Figure 2. Rescaled perturbative correction in g^2 to the visit probability $\mathcal{Q}(x_1, t)$ of Brownian Motion driven by correlated noise (ATBM, cf. Eq. (26)). The **left** plot shows the result for fixed time, $\mathcal{Q}(x_1, t = 1)$, the **right** plot for fixed distance, $\mathcal{Q}(x_1 = 1, t)$. The **inset of the left plot** shows the visit probability $\mathcal{Q}(x_1, t = 1)$ over distance for simple Brownian Motion ($g^2 = 0$, black line) as well as ATBM for $\beta = 1.0$ and $g^2 = 0.25$ (green dashed line), or $g^2 = 0.5$ (bright green dot-dashed line) respectively. The **inset of the right plot** shows the complement of the corresponding visit probability $1 - \mathcal{Q}(x_1 = 1, t)$ over time, with identical parameters and symbols. The **left (right) main panel** shows the rescaled correction to the visit probability over distance x_1 (rescaled time βt) for three different values of, from top to bottom, $\beta = 2.0$ (red/orange), $\beta = 1.0$ (green), and $\beta = 0.5$ (blue). Plot marks indicate the result obtained from simulation for either $g^2 = 0.25$ (circles) or $g^2 = 0.5$ (crosses). The solid lines indicate our predictions to first leading order in g^2 obtained by calculating the result of Eq. (30) (cf. Eq. (G1)), and numerically inverting the Fourier transform. All simulations used $D_x = D_y = 1$, and $\geq 10^6$ realisations.

$$\mathcal{Q}(x, \omega; g) = \mathcal{Q}^{(0)}(x, \omega) \left[1 + \frac{g^2}{D_x} \left(\frac{\int dt e^{-i\omega t} \Upsilon(t) \partial_t T^{(0)}(x, t)}{T^{(0)}(x, \omega)} - \frac{\int dt e^{-i\omega t} \Upsilon(t) \partial_t R^{(0)}(x, t)}{R^{(0)}(x, \omega)} \right) \right] + \mathcal{O}(g^3) \quad (30)$$

This relation illuminates the relation between the correction to the Fourier-transformed visit probability and the correlation function of the driving noise. To obtain the visit probabilities, and derive extreme event distributions, in real time (cf. Eqs. (5), (6), (7)), numerical integration will be necessary in most cases.

For exponentially correlated driving noise, such as “coloured” or telegraphic noise, we have $C_2(t) = D_x \beta e^{-\beta|t|}$, Eq. (18), for some noise strength D_x and timescale of relaxation β^{-1} . The corresponding time-stretch function is

$$\Upsilon(t) = \frac{D_y}{\beta} (e^{-\beta t} + \beta t - 1) \quad (31)$$

From this function alone, one can read off that for large times the driving noise effectively shifts the diffusion constant by $D_x \rightarrow D_x + g^2 D_y$. At short time-scales ($t \lesssim \beta^{-1}$), however, the correction is non-trivial.

We can further verify the validity of the expansion of the trace function $\mathcal{Q}(x, \omega; g)$, Eq. (30), by numerically inverting the Fourier-transform and compare to Monte-Carlo simulations of the process Eq. (26). To this end, we estimate numerically the probability that x_t has reached x_1 , at some given t and parameters such as g , D_x and D_y , and subtract from it the exact result $\mathcal{Q}(x, t; g = 0)$.

Plotting this difference over g^2 produces an estimate of the correction of $\mathcal{Q}(x, t; 0)$ to $\mathcal{Q}(x, t, g)$, described by Eq. (30) to leading order (see Eq. (G1) for explicit result). Fig. 2 shows this numerically estimated correction together with the inverted correction Eq. (30).

The persistence exponent θ is defined as the tail exponent of the survival probability $\mathbb{P}_{\text{surv}}(x, t) = 1 - \mathcal{Q}(x, t) \sim t^{-\theta}$ [4, 6]. It is also contained in the small ω expansion of the trace as $(-i\omega)^{-1} - \mathcal{Q}(x, \omega) \sim \omega^{\theta-1}$. Evaluating Eq. (30) using the time-stretch function (31) shows that the Markovian result of $\theta = \frac{1}{2}$ [4] does not acquire corrections.

Discussion, Conclusion, Outlook— In the present work we have established a method to compute the visit probability (the complement of the survival probability) for random motion in a one-dimensional potential, as defined in Eq. (17). By mapping the problem to a field-theory we systematically compute corrections to the Markovian result (16) to any order in the coupling g . The leading order correction is of the form (24), which involves the g^2 -corrected transition probability given in (25). Generally, to compute contribution to order g^n , it is sufficient to know the Markovian transition probability and the n -point function of the driving noise y_t . In the absence of an

external potential, the expressions reduce to (30) which depends on the twice-integrated driving noise correlation $\Upsilon(t)$, Eq. (27).

By casting the problem in a field-theoretic language, we replaced the single degree of freedom by a field φ representing the full density. This allows us to extend the model to the case of many, potentially interacting, random walkers. Also, the Doi-Peliti framework allows for the inclusion of potentials. To the best of our knowledge, this is the first time that both Doi-Peliti and Martin-Siggia-Rose have been used simultaneously to construct an action. Overall, we have established a method which further lays bare the interplay between

non-Markovianness and extreme events in stochastic processes.

Acknowledgements— BW and GP would like to thank the Francis Crick Institute for their hospitality. BW would like to thank Andrea Gambassi for insightful discussions and comments. BW acknowledges financial support from MIUR-PRIN project “Coarse-grained description for non-equilibrium systems and transport phenomena (CO-NEST)” n. 201798CZL. GS was supported by the Francis Crick Institute which receives its core funding from Cancer Research UK (FC001317), the UK Medical Research Council (FC001317), and the Wellcome Trust (FC001317).

-
- [1] R. Zwanzig, Ensemble method in the theory of irreversibility, *J. Chem. Phys.* **33**, 1338 (1960).
- [2] F. Haake, Statistical treatment of open systems by generalized master equations, in *Quantum Statistics in Optics and Solid-State Physics* (Springer, Berlin, Heidelberg, 1973) pp. 98–168.
- [3] R. Zwanzig, *Nonequilibrium Statistical Mechanics* (Oxford University Press, 2001).
- [4] S. N. Majumdar, Persistence in nonequilibrium systems, *Curr. Sci.* **77**, 370 (1999).
- [5] A. J. Bray, S. N. Majumdar, and G. Schehr, Persistence and first-passage properties in nonequilibrium systems, *Adv. Phys.* **62**, 225 (2013).
- [6] F. Aurzada and T. Simon, Persistence probabilities and exponents, in *Lévy Matters V*, Lecture Notes in Mathematics, Vol. 2149 (Springer, 2015) Chap. 3, pp. 183–224.
- [7] E. Schrödinger, Zur Theorie der Fall- und Steigversuche an Teilchen mit Brownscher Bewegung, *Z. Phys.* **16**, 289 (1915).
- [8] H. E. Daniels and F. Smithies, The probability distribution of the extent of a random chain, *Math. Proc. Camb. Philos. Soc.* **37**, 244–251 (1941).
- [9] B. Gnedenko, Sur la distribution limite du terme maximum d’une série aléatoire, *Ann. Math.* **44**, 423 (1943).
- [10] D. A. Darling and A. J. F. Siegert, The First Passage Problem for a Continuous Markov Process, *Ann. Math. Stat.* **24**, 624 (1953).
- [11] E. J. Gumbel, *Statistics of Extremes* (Columbia University Press, 1958).
- [12] R. Metzler, G. Oshanin, and S. Redner, *First-Passage Phenomena and Their Applications* (World Scientific, 2014).
- [13] S. N. Majumdar, A. Pal, and G. Schehr, Extreme value statistics of correlated random variables: a pedagogical review, *Phys. Rep.* **840**, 10.1016/j.physrep.2019.10.005 (2020), arXiv: 1910.10667.
- [14] S. N. Majumdar, A. J. Bray, S. J. Cornell, and C. Sire, Global persistence exponent for nonequilibrium critical dynamics, *Phys. Rev. Lett.* **77**, 3704 (1996).
- [15] K. Oerding, S. J. Cornell, and A. J. Bray, Non-markovian persistence and nonequilibrium critical dynamics, *Phys. Rev. E* **56**, R25 (1997).
- [16] K. J. Wiese, S. N. Majumdar, and A. Rosso, Perturbation theory for fractional brownian motion in presence of absorbing boundaries, *Phys. Rev. E* **83**, 061141 (2011).
- [17] M. Arutkin, B. Walter, and K. J. Wiese, Extreme events for fractional brownian motion with drift: Theory and numerical validation, *Phys. Rev. E* **102**, 022102 (2020).
- [18] K. Malakar, V. Jemseena, A. Kundu, K. Vijay Kumar, S. Sabhapandit, S. N. Majumdar, S. Redner, and A. Dhar, Steady state, relaxation and first-passage properties of a run-and-tumble particle in one-dimension, *J. Stat. Mech. Theory Exp.* **2018**, 043215 (2018).
- [19] F. J. Sevilla, R. F. Rodríguez, and J. R. Gomez-Solano, Generalized ornstein-uhlenbeck model for active motion, *Phys. Rev. E* **100**, 032123 (2019).
- [20] L. Dabelow, S. Bo, and R. Eichhorn, Irreversibility in active matter systems: Fluctuation theorem and mutual information, *Phys. Rev. X* **9**, 021009 (2019).
- [21] A. Shee, A. Dhar, and D. Chaudhuri, Active brownian particles: mapping to equilibrium polymers and exact computation of moments, *Soft Matter* **16**, 4776 (2020).
- [22] D. Martin and T. A. de Pirey, Aoup in the presence of brownian noise: a perturbative approach, *J. Stat. Mech. Theory Exp.* , 043205 (2021).
- [23] J. Luczka, Non-Markovian stochastic processes: Colored noise, *Chaos* **15**, 026107 (2005).
- [24] L. Caprini and M. B. U. Marconi, Active particles under confinement and effective force generation among surfaces, *Soft Matter* **14**, 9044 (2018).
- [25] L. Caprini, U. M. B. Marconi, A. Puglisi, and A. Vulpiani, The entropy production of Ornstein–Uhlenbeck active particles: a path integral method for correlations, *J. Stat. Mech. Theory Exp.* **2019**, 053203 (2019).
- [26] B. Walter, G. Pruessner, and G. Salbreux, First passage time distribution of active thermal particles in potentials, *Phys. Rev. Research* **3**, 013075 (2021).
- [27] A. J. F. Siegert, On the First Passage Time Probability Problem, *Phys. Rev.* **81**, 617 (1951).
- [28] M. Doi, Second quantization representation for classical many-particle system, *J. Phys. A: Math. Gen.* **9**, 1465 (1976).
- [29] L. Peliti, Path integral approach to birth-death processes on a lattice, *J. Phys. (Paris)* **46**, 1469 (1985).
- [30] P. C. Martin, E. D. Siggia, and H. A. Rose, Statistical dynamics of classical systems, *Phys. Rev. A* **8**, 423 (1973).
- [31] N. G. v. Kampen, *Stochastic processes in physics and chemistry*, 3rd ed. (Elsevier, 2007).
- [32] R. Garcia-Millan and G. Pruessner, Tba (2021).
- [33] U. C. Täuber, M. Howard, and B. P. Vollmayr-Lee, Ap-

- lications of field-theoretic renormalization group methods to reaction-diffusion problems, *J. Phys. A: Math. Gen.* **38**, R79 (2005).
- [34] J. Cardy, Reaction-diffusion processes (2006), accessed 8 Jul 2014, preprint of [40].
- [35] I. Bordeu, S. Amarteifio, R. Garcia-Millan, B. Walter, N. Wei, and G. Pruessner, Volume explored by a branching random walk on general graphs, *Sci. Rep.* **9**, 15590 (2019), [arXiv:1909.00471](https://arxiv.org/abs/1909.00471).
- [36] S. Nekovar and G. Pruessner, A field-theoretic approach to the wiener sausage, *J. Stat. Phys.* **163**, 604 (2016), [arXiv:1407.7419](https://arxiv.org/abs/1407.7419).
- [37] S. Amarteifio, *Field theoretic formulation and empirical tracking of spatial processes*, *Ph.D. thesis*, Imperial College London (2019).
- [38] J. Cardy, Field theory and nonequilibrium statistical mechanics (1999), lectures presented as part of the Troisieme Cycle de la Suisse Romande.
- [39] W. Horsthemke and R. Lefever, *Noise-induced transitions: Theory and applications in physics, chemistry, and biology*, 2nd ed. (Springer, Berlin, 2006).
- [40] J. Cardy, Reaction-diffusion processes, in *Nonequilibrium Statistical Mechanics and Turbulence*, edited by S. Nazarenko and O. V. Zaboronki (Cambridge University Press, Cambridge, UK, 2008) pp. 108–161, London Mathematical Society Lecture Note Series: 355, preprint available from <http://www-thphys.physics.ox.ac.uk/people/JohnCardy/warwick.pdf>.
- [41] H. Risken, *The Fokker-Planck Equation* (Springer, 1984).
- [42] U. C. Täuber, *Critical dynamics* (Cambridge University Press, Cambridge, UK, 2014) pp. i–xvi,1–511.
- [43] M. Le Bellac, *Quantum and Statistical Field Theory [Phenomenes critiques aux champs de jauge, English]* (Oxford University Press, New York, NY, USA, 1991) translated by G. Barton.
- [44] Wolfram Research, Inc., *Mathematica, Version 12.3.1* (2021), Champaign, IL.
- [45] I. S. Gradshteyn and I. Ryzhik, *Table of Integrals, Series, and Products*, 7th ed. (Academic Press, 2007).

Appendix A: Tracing mechanism

The visit probability for Markovian processes (cf. (1)), given in (9), is a result that can be derived in various ways (indirectly, via the first-passage time distribution, $\partial_t \mathcal{Q}(x, t)$, this result has been found in, eg. , [10] using a renewal type approach). Here, we derived the result by taking the continuum limit of a discrete reaction-diffusion process designed to track visits, which we refer to as “tracing mechanism” and which has been introduced in [35, 36].

To describe the tracing mechanism, we consider a coarse-grained version \mathfrak{r}_t of the stochastic process x_t of Eq. (1), which takes values only on a lattice $\delta_a \mathbb{Z}$ where δ_a is the lattice-spacing, so that formally $\mathfrak{r}_t = \delta_a [\delta_a^{-1} x_t]$ where $[x]$ rounds to the nearest integer. At any time, the random walker attempts to deposit a *trace* at \mathfrak{r}_t with Poissonian rate proportional to γ . Each lattice site, however, has a “carrying capacity” n_0 which limits the number of trace particles that can be deposited at this site. If at a site n_0 trace particles have already been deposited, any further deposition is suppressed. Hence, the number of trace particles deposited at any lattice site is an integer bound above by n_0 . Taking $\gamma \rightarrow \infty$, the particle deterministically deposits trace particles at any site visited for the first time. In the limit of $\delta_a \rightarrow 0$, the process \mathfrak{r}_t tends to x_t , and the expected number of trace particles at a site, divided by n_0 , converges to $\mathcal{Q}(x, t)$.

Cast into the language of reaction diffusion processes, we have



where particles of species W (“walkers”) deposit particles of species T (“traces”) at rate γ , provided their number does not surpass the carrying capacity n_0 . Meanwhile W diffuses according to (a discretised form of) (1), T remains at a given site and “evaporates” with rate ε , later sent to zero.

The Doi-Peliti formalism [28, 29] describes the continuum limit of particle densities in a reaction-diffusion system, such as defined in Eqs. (A1), (A2), by mapping the problem onto a non-equilibrium field theory, where each particle species corresponds to a pair of fields. Here (see [36] for details), the walkers are mapped to $\varphi(x, t), \tilde{\varphi}(x, t)$ (referred to as annihilation and creation fields, respectively), and the trace particles to $\psi(x, t), \tilde{\psi}(x, t)$. As shown in [35, 36], the joint distribution of the four fields then follows from the Doi Peliti framework to be distributed according to the action given in (3), (10), and (11).

Appendix B: Field-theoretic Calculation of Markovian visit probability

We derive Eq. (16), the expression for the visit probability in the Markovian case. First, we consider the field theory in the case of $\gamma = 0$, when the probability measure (8) is Gaussian.

We introduce the forward and backward operators $\mathcal{L}, \mathcal{L}^\dagger$,

$$\mathcal{L}(x) = V''(x) + V'(x)\partial_x + D_x\partial_x^2, \quad (\text{B1})$$

$$\mathcal{L}^\dagger(x) = -V'(x)\partial_x + D_x\partial_x^2 \quad (\text{B2})$$

associated to (1) and generating the corresponding Fokker Planck Equation

$$\begin{aligned} \partial_t T(x, t) &= \mathcal{L}T(x, t) \\ T(x, t = t_0) &= \delta(x - x_0) \end{aligned} \quad (\text{B3})$$

with $T(x, t)$ the transition probability of the process. The forward and backward operator have a set of eigenfunctions

$$\mathcal{L}u_n(x) = -\lambda_n u_n(x) \quad (\text{B4})$$

$$\mathcal{L}^\dagger v_n(x) = -\lambda_n v_n(x) \quad (\text{B5})$$

with eigenvalues $0 \leq \lambda_0 < \lambda_1 \dots$. The eigenfunctions are L^2 -normalised to satisfy the orthonormal relation

$$\int dx u_m(x)v_n(x) = \delta_{mn}, \quad (\text{B6})$$

and since they form a complete set in L^2 they further satisfy [41]

$$\sum_n v_n(x_1)u_n(x_2) = \delta(x_1 - x_2). \quad (\text{B7})$$

Thus, every field $\varphi, \tilde{\varphi}, \psi, \tilde{\psi}$ has a unique decomposition into the $u_n(x), v_n(x)$ in space. Together with a Fourier transform in time, we then write

$$\varphi(x, t) = \int \tilde{d}\omega \sum_k \varphi_k(\omega) u_k(x) e^{-i\omega t} \quad (\text{B8})$$

$$\tilde{\varphi}(x, t) = \int \tilde{d}\omega \sum_k \tilde{\varphi}_k(\omega) v_k(x) e^{-i\omega t}, \quad (\text{B9})$$

and analogously for $\psi, \tilde{\psi}$ with coefficients $\psi_k(\omega), \tilde{\psi}_k(\omega')$, respectively. This *mode transform* diagonalises the non-perturbative parts of the action, \mathcal{S}_φ and \mathcal{S}_ψ (cf. Eq. (8)), which read

$$\mathcal{S}_\varphi[\varphi, \tilde{\varphi}] = \int \tilde{d}\omega \sum_n \tilde{\varphi}_n(-\omega) (-i\omega + \lambda_n) \varphi_n(\omega) \quad (\text{B10})$$

$$\mathcal{S}_\psi[\psi, \tilde{\psi}] = \int \tilde{d}\omega \sum_n \tilde{\psi}_n(-\omega) (-i\omega + \varepsilon) \psi_n(\omega). \quad (\text{B11})$$

For $\gamma = 0$, the measure in Eq. (8) is Gaussian and the (Fourier transformed) bare propagators of both fields, $\langle \varphi \tilde{\varphi} \rangle$ and $\langle \psi \tilde{\psi} \rangle$, therefore immediately follow from Eqs. (B10) and (B11) using standard path integral techniques [42],

$$\langle \varphi_n(\omega') \tilde{\varphi}_m(\omega) \rangle = \frac{\delta_{m,n} \delta(\omega + \omega')}{-i\omega' + \lambda_n} = \underbrace{(m, \omega') \quad (n, \omega)} \quad (\text{B12})$$

$$\langle \psi_n(\omega') \tilde{\psi}_m(\omega) \rangle = \frac{\delta_{m,n} \delta(\omega + \omega')}{-i\omega' + \varepsilon} = \underbrace{(m, \omega') \quad (n, \omega)}_{\text{wavy line}}, \quad (\text{B13})$$

where we introduced a diagrammatic representation for both bare propagators. These propagators are commonly interpreted as the (linear) response functions [42]. Using Eq. (4), and transforming back into real space and time using Eqs. (B8) and (B9), we obtain the transition probability

$$T(x, t) = \sum_n v_n(x_0) u_n(x) e^{-\lambda_n(t-t_0)} \Theta(t - t_0) \quad (\text{B14})$$

where $\Theta(t)$ is the Heaviside Θ -function. Crucially, we made use of the property [38, 42]

$$\langle \varphi \rangle_S = 0 \quad (\text{B15})$$

such that $\langle \varphi(1 + \tilde{\varphi}) \rangle = \langle \varphi \tilde{\varphi} \rangle$.

We next consider the expectation (4) in the case of $\gamma \neq 0$ when the non-linear contributions of \mathcal{S}_γ , Eq. (11), enter. Each of the four vertices is diagrammatically represented as

$$\begin{array}{cccc} \tau & \sigma & -\lambda & -\kappa \\ \text{---} & \text{---} & \text{---} & \text{---} \\ \text{wavy} & \text{wavy} & \text{wavy} & \text{wavy} \end{array} \quad (\text{B16})$$

and enters into the action multiplied by γ . It follows that the diagrammatic expansion of the trace function (9) is

$$\mathcal{Q}(x, t) = n_0^{-1} \lim_{\gamma \rightarrow \infty} \begin{array}{c} (x, t) \\ \text{---} \\ \text{wavy} \bullet \text{---} \\ (x_0, t_0) \end{array} \quad (\text{B17})$$

$$\int dt e^{i\omega t} \mathcal{Q}(x, t) = n_0^{-1} \langle \psi(x) \tilde{\psi}(x) \rangle \left(\lim_{\gamma \rightarrow \infty} \tau_R(\omega) \right) \langle \varphi(x, \omega) \tilde{\varphi}(x_0, \omega) \rangle \quad (\text{B18})$$

$$= n_0^{-1} \frac{1}{-i\omega + \varepsilon} \left(\lim_{\gamma \rightarrow \infty} \tau_R(\omega) \right) T(x_0, x, \omega) \quad (\text{B19})$$

where the central dot in the diagram stands for the renormalised coupling τ_R , and $T(x_0, x, \omega)$ is the Fourier transform of the transition probability. This renormalisation of τ is given by the diagrammatic expansion of the amputated vertex

$$\tau_R = \bullet = \gamma \begin{array}{c} \tau \\ \text{---} \\ \text{wavy} \end{array} + \gamma^2 \begin{array}{c} -\lambda \ \sigma \\ \text{---} \\ \text{wavy} \end{array} + \gamma^3 \begin{array}{c} -\lambda - \kappa \ \sigma \\ \text{---} \\ \text{wavy} \end{array} + \dots \quad (\text{B20})$$

The only diagrams contributing to this expansions are chains of the loop-diagram , referred to in the following as a "bubble". Considering the expansion in Fourier and mode transform, Eqs. (B8) and (B9) (App. D for details), each diagram factorises into a product over the bubbles and can hence be evaluated using a geometric or Dyson sum (App. D for derivation) resulting in

$$\tau_R(\omega_1) = \frac{\gamma \tau}{1 + \gamma \kappa R(x_1, \omega_1)} \quad (\text{B21})$$

such that the effective trace function, Fourier transformed, is

$$\int dt e^{i\omega t} \mathcal{Q}(x, t) = \lim_{\gamma \rightarrow \infty} \frac{1}{-i\omega + \varepsilon} \frac{\gamma \tau n_0^{-1}}{1 + \gamma \kappa R(x_1, \omega + i\varepsilon)} T(x_0, x_1, \omega) = \frac{1}{-i\omega + \varepsilon} \frac{T(x_0, x_1, \omega)}{R(x_1, \omega + i\varepsilon)} \quad (\text{B22})$$

where we made use of time-translational invariance to write the Fourier-transform in one frequency only. The couplings τ/κ in Eq. (B21) cancel with n_0^{-1} in the definition of $\mathcal{Q}(x, t)$, Eq. (9). This then leads to the central Markovian result for the trace function

$$\mathcal{Q}(x, t) = \int d\omega e^{-i\omega t} \frac{T(x_0, x_1, \omega)}{(-i\omega)R(x_1, \omega)} \quad (\text{B23})$$

where we have tacitly taken the limit $\varepsilon \rightarrow 0$.

Appendix C: Visit probability for driven process

In this appendix, we provide some technical details to the derivation of the key result 24 and 25 which together provide the visit probability for non-Markovian processes of the form (17).

There are three technical steps: First, we consider the perturbative correction of the visit probability in the presence of a fixed, but random, realisation of the driving noise y_t . Secondly, we average over all such realisations of y_t . This then leads to a large set of correction terms which we interpret diagrammatically and which, thirdly, we evaluate to leading perturbative order.

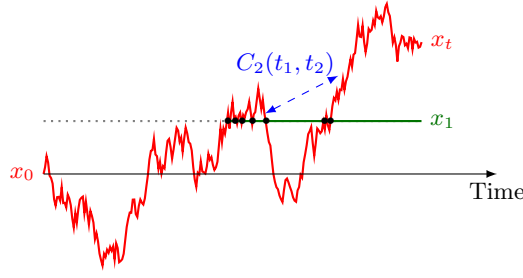


Figure 3. The random walker x_t (red solid path) travels from $x_0 < x_1$ to $x_t > x_1$, thereby passing x_1 (green solid line) infinitely often (black dots). If the random walker is additionally driven by self-correlated noise (cf. Eq. (17)), this induces correlations between increments at any different times t_1, t_2 (blue dashed line). Meanwhile the perturbative expansion in γ (cf. Eq. (14)) tracks the probability of all possible transitions $T(x_1, t)$ and subsequent returns from x_0 to x_1 , the second perturbative expansion in g includes the effect of correlated increments. If $g = 0$, the Markovian case, the process undergoes renewal at every return at x_1 , thus rendering the results such as Eq. (B22) *exact*.

1. Averaging general observables over driving noise

The presence of the autocorrelated driving noise y_t affects the transition and return probabilities of the random walker x_t (see Fig. 3). Conditioned on a fixed realisation of y_t , the forward operator (cf. Eqs. (1), (B3), (B1) and (17)) is shifted by

$$\mathcal{L} \mapsto \mathcal{L} + gy_t \partial_x \varphi(x, t) \quad (\text{C1})$$

Hence, the y_t -conditioned random walker action Eq. (3), which is essentially of the form $\tilde{\varphi}(\partial_t - \mathcal{L})\varphi$, is shifted also,

$$\mathcal{S}_\varphi[y_t] = \iint dx dt \tilde{\varphi}(\partial_t - \mathcal{L} - gy_t \partial_x)\varphi. \quad (\text{C2})$$

To obtain the y -averaged joint distribution of the four fields, one needs to evaluate (Eqs. (8), (19))

$$\overline{\mathcal{P}[\varphi, \tilde{\varphi}, \psi, \tilde{\psi}]} = \lim_{\gamma \rightarrow \infty} \int \mathcal{D}[y_t] \exp\left(-\mathcal{S}_\varphi[\varphi, \tilde{\varphi}] - \mathcal{S}_\psi[\psi, \tilde{\psi}] + \gamma \mathcal{S}_\gamma[\varphi, \tilde{\varphi}, \psi, \tilde{\psi}] + \iint gy_t \tilde{\varphi} \partial_x \varphi\right) \mathcal{P}[y_t], \quad (\text{C3})$$

where $gy_t \tilde{\varphi} \partial_x \varphi$ may be interpreted as a new vertex, (see Eq. (23)). Whilst we were able to compute the result exactly in γ , we need to resort to perturbative methods to approximate in small couplings g . Although the path-integral in (19) appears to require complete knowledge of the full path measure $\mathcal{P}[y_t]$ of the driving noise y_t , we can relax this requirement by introducing the normalised partition function (or moment generating function) of y_t ,

$$\mathcal{Z}_y[g \cdot j_t] = \int \mathcal{D}[y_t] \exp\left(g \int dt j_t y_t\right) \mathcal{P}[y_t] \quad (\text{C4})$$

$$= 1 + \frac{1}{2}g^2 \iint dt_1 dt_2 j_{t_1} C(t_2 - t_1) j_{t_2} + \mathcal{O}(g^3) \quad (\text{C5})$$

where we ignore terms of higher perturbative order. We may thus replace the y_t -integration in Eq. (19) by inserting $\mathcal{Z}_y[g \int dx dt \tilde{\varphi} \partial_x \varphi]$ into expectations over the fields and consequently evaluate double averages via

$$\overline{\langle \bullet \rangle}_{\mathcal{S}+gy} = \left\langle \bullet \cdot \mathcal{Z}_y \left[g \iint dx dt \tilde{\varphi} \partial_x \varphi \right] \right\rangle_{\mathcal{S}}. \quad (\text{C6})$$

For example, the transition probability, averaged over all driving noises y_t , acquires a correction term which up to g^2 reads

$$T(x_1, t) = \langle \varphi(x_1, t) \tilde{\varphi}(x_0, 0) \rangle \quad (\text{C7})$$

$$+ g^2 \iint dy_1 ds_1 dy_2 ds_2 C_2(s_2 - s_1) \langle \varphi(x_1, t) \tilde{\varphi}(y_1, s_1) \partial_{y_1} \varphi(y_1, s_1) \tilde{\varphi}(y_2, s_2) \partial_{y_2} \varphi(y_2, s_2) \tilde{\varphi}(x_0, 0) \rangle_{\mathcal{S}} + \mathcal{O}(g^4) \quad (\text{C8})$$

Crucially, the averages $\langle \bullet \rangle_{\mathcal{S}; \gamma=0}$ are taken over Gaussian random variables since for $\gamma = 0$ the path action (Eq. (8)) is bilinear. Thus, Wick's theorem (eg. [43]) applies and all averages in Eq. (D2) decompose into products of two-point functions. The only such Gaussian two-point functions which do not vanish are

$$\langle \varphi(z_1, \omega_1) \tilde{\varphi}(z_0, \omega_0) \rangle_{\mathcal{S}; \gamma=0} = T(z_0, z_1; \omega_1) \delta(\omega_0 + \omega_1) = \int \tilde{d}\omega_1 e^{i\omega_1(t-t_0)} T(z_0, z_1; t) \delta(\omega_0 + \omega_1) \quad (\text{D3})$$

$$\langle \psi(z_1, \omega_1) \tilde{\psi}(z_0, \omega_0) \rangle_{\mathcal{S}; \gamma=0} = \frac{\delta(z_1 - z_0) \delta(\omega_0 + \omega_1)}{-i\omega_1 + \varepsilon} = \iint \tilde{d}\omega_0 \tilde{d}\omega_1 e^{i\omega_1 t + i\omega_0 t_0} \Theta(t - t_0) \delta(z_1 - z_0) e^{-\varepsilon(t-t_0)} \quad (\text{D4})$$

The second correlator intuitively characterises the behaviour of the trace which, once deposited at z_0 at time t_0 , remains there for an infinitely long time, as $\varepsilon \rightarrow 0$. Equipped with these correlators, the non-vanishing contributions to the averages appearing in Eq. (D2) are, following Wick's theorem,

$$\begin{aligned} n_0^{-1} \gamma \tau \iint dz \tilde{d}\omega' \langle \psi(x_1, \omega_1) \tilde{\psi}(z, \omega') \varphi(z, \omega') \tilde{\varphi}(x_0, \omega_0) \rangle_{\mathcal{S}; \gamma=0} &= n_0^{-1} \gamma \tau \iint dz \tilde{d}\omega' \frac{\delta(x_1 - z) \delta(\omega_1 + \omega')}{-i\omega_1 + \varepsilon} T(x_0, z, \omega') \delta(\omega' + \omega_0) \\ &= n_0^{-1} \gamma \tau \frac{T(x_0, x_1, -\omega_1)}{-i\omega_1 + \varepsilon} \delta(\omega_0 - \omega_1), \end{aligned} \quad (\text{D5})$$

and to second order,

$$-n_0^{-1} \gamma^2 \lambda \sigma \iint dz_1 dz_2 \tilde{d}\omega'_1 \tilde{d}\omega'_2 \tilde{d}\omega''_1 \tilde{d}\omega''_2 \quad (\text{D6})$$

$$\times \langle \psi(x_1, \omega_1) \tilde{\psi}(z_1, -\omega'_1 - \omega''_1) \psi(z_1, \omega_1'') \varphi(z_1, \omega_1') \tilde{\psi}(z_2, \omega_2'') \tilde{\varphi}(z_2, \omega_2') \varphi(z_2, -\omega'_2 - \omega''_2) \tilde{\varphi}(x_0, \omega_0) \rangle_{\mathcal{S}; \gamma=0} \quad (\text{D7})$$

$$= -n_0^{-1} \gamma^2 \lambda \sigma \frac{1}{-i\omega_1 + \varepsilon} \int \tilde{d}\omega''_2 \frac{R(x_1, x_1, \omega_1 - \omega''_2)}{-i\omega''_1 + \varepsilon} T(x_0, x_1, \omega_0) \delta(\omega_0 + \omega_1) \quad (\text{D8})$$

$$= -n_0^{-1} \gamma^2 \lambda \sigma R(x_1, \omega_1 + i\varepsilon) \frac{T(x_0, x_1, \omega_0)}{-i\omega_1 + \varepsilon} \delta(\omega_0 + \omega_1), \quad (\text{D9})$$

where in the first equality we used the definition of the return probability to abbreviate

$$\iint dz_1 dz_2 \delta(x_1 - z_1) \delta(z_1 - z_2) T(z_1, z_2, \omega) = R(x_1, \omega), \quad (\text{D10})$$

and in the second equality used Cauchy's residue formula to solve the integral by evaluating the residue of the simple pole at $\omega''_2 = -i\varepsilon$.

Since both correlators in Eq. (D3) are proportional to $\delta(\omega_0 + \omega_1)$, all higher order expansion terms factorise, after integrating over the internal frequencies, into a product over amputated one-loop bubble diagrams (ie. interpreted here as a function of external parameters z_1, ω_1 and z_2, ω_2 , respectively) which by analogous reasoning to the calculation above evaluate as

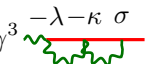
$$z_1, \omega_1 \text{  } z_2, \omega_2 = \gamma^2 \lambda \sigma R(z_1, \omega_1 + i\varepsilon) \delta(\omega_1 + \omega_2) \delta(z_1 - z_2). \quad (\text{D11})$$

The bubble diagram graphically encodes the probability of a particle depositing a trace and then returning to it, in other words a "time-ordered" return probability: The green wiggly line may be understood as the trace which once placed remains immobile, meanwhile the red solid line represents the diffusing, and returning, walker. Likewise, the higher order diagrams in Eq. (14) may be interpreted as repeated returns to x_1 .

Returning to Eq. (14), the renormalised τ coupling, τ_R , is the effective factor satisfying

$$\langle \psi(x_1, \omega_1) \tilde{\varphi}(x_0, \omega_0) \rangle_{\mathcal{S}} = \frac{1}{-i\omega_1 + \varepsilon} \tau_R(\omega_1) T(x_0, x_1, -\omega_0) \delta(\omega_0 + \omega_1) \quad (\text{D12})$$

and collecting the factors generated by the terms in Eq. (D2), and evaluated using Eq. (D11), one obtains

$$\tau_R(\omega_1) = \gamma \text{  } + \gamma^2 \text{  } + \gamma^3 \text{  } + \dots \quad (\text{D13})$$

$$= \left[\gamma \tau - \gamma^2 \lambda \sigma R(x_1, \omega_1 + i\varepsilon) + \gamma^3 \lambda \sigma \kappa (R(x_1, \omega_1 + i\varepsilon))^2 - \gamma^4 c \sigma \kappa^2 (R(x_1, \omega_1 + i\varepsilon))^3 + \dots \right] \delta(\omega_0 + \omega_1) \quad (\text{D14})$$

This series can be resummed using the geometric series, in field theory often referred to as Dyson summation [43]. Rearranging the sum gives

$$\tau_R(\omega_1) = \left[\gamma\tau + \gamma \frac{\lambda\sigma}{\kappa} \sum_{r=1}^{\infty} (-\gamma\kappa R(x_1, \omega_1 + i\varepsilon))^r \right] \quad (\text{D15})$$

$$= \left[\gamma\tau + \gamma \frac{\lambda\sigma}{\kappa} \sum_{r=0}^{\infty} (-\gamma\kappa R(x_1, \omega_1 + i\varepsilon))^r - \gamma \frac{c\sigma}{\kappa} \right] \quad (\text{D16})$$

$$= \left[\frac{\gamma\tau}{1 + \gamma\kappa R(x_1, \omega_1 + i\varepsilon)} + \gamma \underbrace{\left(\tau - \frac{c\sigma}{\kappa} \right)}_{=0} \right] \quad (\text{D17})$$

$$= \frac{\gamma\tau}{1 + \gamma\kappa R(x_1, \omega_1 + i\varepsilon)} \quad (\text{D18})$$

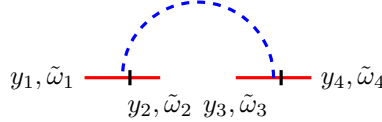
where we made use of the bare values given in Eq. (11), ie. replaced σ with τ and used $\lambda = \kappa$ at bare level. This vertex interpolates the physical pictures for $\gamma = 0$, where no deposition takes place ($\tau_R = 0$), and $\gamma \rightarrow \infty$, where every newly visited site gets marked immediately by a deposited trace. For $\gamma \rightarrow \infty$, the coupling tends to

$$\lim_{\gamma \rightarrow \infty} \tau_R(\omega_1) = \frac{n_0}{R(x_1, \omega_1 + i\varepsilon)}, \quad (\text{D19})$$

using $n_0 = \tau/\kappa$.

Appendix E: Derivation of four non-Markovian correction terms to trace function

When expanding the nonlinear action in Eq. (C12) to all orders in γ and to $\mathcal{O}(g^2)$, the nonvanishing contribution of joint perturbative order $\gamma^n g^2$ is obtained by inserting the (Fourier-transformed) g^2 -decoration



$$y_1, \tilde{\omega}_1 \text{---} y_2, \tilde{\omega}_2 \text{---} y_3, \tilde{\omega}_3 \text{---} y_4, \tilde{\omega}_4 \quad (\text{E1})$$

$$= \iint d^d \tilde{\omega}_1 \dots d^d \tilde{\omega}_4 dy_1 \dots dy_4 \tilde{\varphi}(y_1, \tilde{\omega}_1) \partial_{y_2} \varphi(y_2, \tilde{\omega}_2) C_2(\tilde{\omega}_3 + \tilde{\omega}_4) \tilde{\varphi}(y_3, \tilde{\omega}_3) \partial_{y_4} \varphi(y_4, \tilde{\omega}_4) \times \delta(\tilde{\omega}_1 + \tilde{\omega}_2 + \tilde{\omega}_3 + \tilde{\omega}_4) \quad (\text{E2})$$

into the expansion of the trace function $\langle \psi \tilde{\varphi} \rangle$ as

$$\mathcal{Q}(x_0, x_1, \omega) \delta(\omega + \omega') \quad (\text{E3})$$

$$= \sum_{n=0}^{\infty} \gamma^{2+n} \int d\tilde{\omega}_1 \dots d\tilde{\omega}_n d\tilde{\omega}_1 \dots d\tilde{\omega}_4 dz_1 \dots dz_n dy_1 \dots dy_4 \quad (\text{E4})$$

$$\left\langle \psi(x_1, \omega) \left(-\lambda \tilde{\psi}(z_1, \omega_1) \tilde{\varphi}(z_1, \omega_1) \psi(z_1, \omega_1) \right) \left(-\kappa \tilde{\varphi}(z_2, \omega_2) \tilde{\psi}(z_2, \omega_2) \varphi(z_2, \omega_2) \psi(z_2, \omega_2) \right) \right. \quad (\text{E5})$$

$$\left. \dots \left(-\kappa \tilde{\varphi}(z_{n-1}, \omega_{n-1}) \tilde{\psi}(z_{n-1}, \omega_{n-1}) \varphi(z_{n-1}, \omega_{n-1}) \psi(z_{n-1}, \omega_{n-1}) \right) \left(\sigma \tilde{\varphi}(z_n, \omega_n) \tilde{\psi}(z_n, \omega_n) \varphi(z_n, \omega_n) \right) \varphi(x_0, \omega') \right. \quad (\text{E6})$$

$$\left. \times g^2 \tilde{\varphi}(y_1, \tilde{\omega}_1) \partial_{y_2} \varphi(y_2, \tilde{\omega}_2) C_2(\tilde{\omega}_3 + \tilde{\omega}_4) \tilde{\varphi}(y_3, \tilde{\omega}_3) \partial_{y_4} \varphi(y_4, \tilde{\omega}_4) \times \delta(\tilde{\omega}_1 + \tilde{\omega}_2 + \tilde{\omega}_3 + \tilde{\omega}_4) \right\}. \quad (\text{E7})$$

As usual, we employ Wick's theorem to evaluate this average over Gaussian random variables: When expanding the average $n_0^{-1} \langle \psi(x_1, \omega) \tilde{\varphi}(x_0, \omega') \rangle$ in powers of γ and g , as shown in Eq. (E3), the resulting coefficients are averages over finite products of $\varphi_1, \dots, \varphi_{j_1}, \tilde{\varphi}_1, \dots, \tilde{\varphi}_{j_2}, \psi_1, \dots, \psi_{j_3}$ and $\tilde{\psi}_1, \dots, \tilde{\psi}_{j_4}$ fields (where $\varphi_i = \varphi(z_i, \omega_i)$ etc.) with respect to the Gaussian measure (defined by the action in Eq. (8) for $\gamma = 0$). Each of those coefficients is evaluated using Wick's theorem, ie.

$$\left\langle \psi_1 \dots \psi_{j_1} \tilde{\psi}_1 \dots \tilde{\psi}_{j_2} \varphi_1 \dots \varphi_{j_3} \tilde{\varphi}_1 \dots \tilde{\varphi}_{j_4} \right\rangle_{S; \gamma=0} = \sum_{\text{pairings } (k_m, \ell_m)} \prod \langle \phi_{k_m} \phi_{\ell_m} \rangle_{S; \gamma=0} \quad (\text{E8})$$

where the sum runs over all possible pairwise pairings of the $j_1 + j_2 + j_3 + j_4$ indices, and we use ϕ in lieu of $\varphi, \tilde{\varphi}, \psi, \tilde{\psi}$ to alleviate notation. Although the number of possible combinations of such pairings is very large, the right hand side of Eq. (E8) drastically simplifies because most of the pairwise averages vanish under the Gaussian average. Again, as in the case of $g = 0$ (cf. App. B), the only non-vanishing Gaussian correlators are those of the form $\langle \varphi \tilde{\varphi} \rangle, \langle \psi \tilde{\psi} \rangle$ as given by Eqs. (D3), (D4). Thus, the sum over averages in Eq. (E3) simplifies into a sum over integrals over products of these two Gaussian propagators. The integrals run over n internal spatial variables z_1, \dots, z_n which stem from the expansion in γ^n , and four internal spatial variables y_1, \dots, y_4 which stem from the expansion in g^2 (and thus are related to the non-Markovian correction). Analogously, the integration also runs over n frequencies $\omega_1, \dots, \omega_n$ stemming from the γ^n -expansion and four frequencies $\tilde{\omega}_1, \dots, \tilde{\omega}_4$ from the g^2 -expansion. The integral over the internal space variables z_1, \dots, z_n , simplifies significantly, since the corresponding $\langle \psi \tilde{\psi} \rangle$ propagators (cf. Eq. (D4)) are proportional to spatial δ -functions. This results in all internal space coordinates to identify as $z_1 = \dots = z_n = x_1$.

The integral over the internal spatial coordinates y_1, \dots, y_4 appearing in the four φ and $\tilde{\varphi}$ fields in Eq. (E3), however, is less trivial as it involves the correlators (“propagators”) of $\langle \varphi \tilde{\varphi} \rangle$. Likewise, the integration over $\tilde{\omega}_1, \dots, \tilde{\omega}_4$, further involves the correlator of the driving noise, $C_2(\tilde{\omega}_3 + \tilde{\omega}_4)$. Hence, the integrals stemming from the g^2 -expansion need to be dealt with more carefully: The four fields $\tilde{\varphi}(y_1, \tilde{\omega}_1) \partial_{y_2} \tilde{\varphi}(y_2, \tilde{\omega}_2) \tilde{\varphi}(y_3, \tilde{\omega}_3) \partial_{y_4} \varphi(y_4, \tilde{\omega}_4)$ appearing in every term of Eq. (E3) have to be paired up (according to Eq. (E8)) with another creation field $\tilde{\varphi}(z_i)$ or annihilation field $\varphi(z_i)$ appearing in Eq. (E3), respectively, in order to have a non-vanishing contribution (cf. Eq. (D3)). Up to permutation of indices, each of these possible combinations (which we refer to as “Wick pairings”, Eq. (E8)) can fundamentally be grouped into four different ways that are best understood diagrammatically: In any case, each of the two $\varphi(y_i) \partial_{y_j} \tilde{\varphi}(y_j)$ attaches via Wick-pairing to a $\varphi(z_k) \tilde{\varphi}(z_\ell)$ field appearing in the terms of Eq. (E3). Concurrently, $\tilde{\varphi}(z_k), \varphi(z_\ell)$, Wick-pair with two other corresponding fields giving rise to connected $\langle \varphi \tilde{\varphi} \rangle$ - “propagators” and so on. Thereby, the Wick-pairing of $\varphi(y_i) \partial_{y_j} \tilde{\varphi}(y_j)$, diagrammatically speaking, splits an existing propagator in the γ^n -expansion into two or, as shown below, in three.

In the expansion to order γ^n , there is one propagator from x_0 to x_1 (*transition*) and n propagators from x_1 to x_1 (*return*) represented by loop diagrams. The g -vertex can thus occur in four different ways, Fig. 1, to be distinguished by whether and how the g -vertex enters into the initial *transition propagator*, --- , in $\text{---} + \text{---} + \dots$, Eq. (D1), or into any of the *return propagators* --- . First, we consider $\mathcal{Q}_1^{(1)}$, I) in Fig. 1, the case of the correlation coupling appearing twice within the same return propagator leading to the diagrammatic sum

$$\mathcal{Q}_1^{(1)}(x_0, x_1, \omega) = n_0^{-1} \lim_{\gamma \rightarrow \infty} \left[-\gamma^2 \text{---} + \gamma^3 \text{---} + \gamma^3 \text{---} + \dots \right] \quad (\text{E9})$$

$$= n_0^{-1} \lim_{\gamma \rightarrow \infty} \left[\gamma^2 \sum_{r=0}^{\infty} \left(\gamma \text{---} \right)^r \times \text{---} \times \sum_{s=0}^{\infty} \left(\gamma \text{---} \right)^s \times \text{---} \right] \quad (\text{E10})$$

$$= -\frac{1}{-i\omega} \frac{T(x_0, x_1)}{(R(x_1, \omega))^2} \iint dy_1 dy_2 d\tilde{\omega} (\partial_{y_1} T(x_1, y_1, \omega)) (\partial_{y_2} T(y_1, y_2, \omega - \tilde{\omega})) T(y_2, x_1, \omega) C_2(\tilde{\omega}) \quad (\text{E11})$$

In the last line, we replaced the geometric sums in Eq. (E10) by the expression found for τ_R in Eq. (D18). To be precise, this is not a matter of trivially renormalising τ to τ_R , as the sums appearing in Eq. (E10) are in fact renormalisations of λ and σ , respectively,

$$-\lambda_R = (-\lambda) \gamma \sum_{r=0}^{\infty} \left(\gamma \text{---} \right)^r = \gamma(-\lambda) + \gamma(-\lambda) \sum_{r=1}^{\infty} (-\gamma \kappa R(x_1, \omega))^r \xrightarrow{\gamma \rightarrow \infty} -\frac{1}{R(x_1, \omega)} \quad (\text{E12})$$

$$\sigma_R = \sigma \gamma \sum_{r=0}^{\infty} \left(\gamma \text{---} \right)^r = \gamma \sigma + \gamma \sigma \sum_{r=1}^{\infty} (-\gamma \kappa R(x_1, \omega))^r \xrightarrow{\gamma \rightarrow \infty} \frac{n_0}{R(x_1, \omega)}, \quad (\text{E13})$$

where again we made use of the definition $n_0 = \sigma \kappa^{-1}$. However, comparing to Eq. (D18), they renormalise identically, as does κ

$$-\kappa_R = (-\kappa) \gamma \sum_{r=0}^{\infty} \left(\gamma \text{---} \right)^r = \gamma(-\kappa) \sum_{r=0}^{\infty} (-\gamma \kappa R(x_1, \omega))^r \xrightarrow{\gamma \rightarrow \infty} -\frac{1}{R(x_1, \omega)} \quad (\text{E14})$$

to be used below.

Another identity entering into expressing $\mathcal{Q}_I^{(1)}$, Eq. (E9), as Eq. (E11), is the key-ingredient of $\mathcal{Q}_I^{(1)}$,

$$(x_1, \omega) \begin{array}{c} \tilde{\omega} \\ \partial_{y_1} \\ \text{---} \\ \partial_{y_2} \end{array} (x_1, \omega) = \iint dy_1 dy_2 d\tilde{\omega} (\partial_{y_1} T(x_1, y_1, \omega)) (\partial_{y_2} T(y_1, y_2, \omega - \tilde{\omega})) T(y_2, x_1, \omega) C_2(\tilde{\omega}) \quad (\text{E15})$$

Considering $\mathcal{Q}_{II}^{(1)}$, shown as II) in Fig. 1, next, the two g -vertices may be inserted into two different return propagators \overleftarrow{g} of a diagram in the expansion Eq. (D1),

$$\mathcal{Q}_{II}^{(1)}(x_0, x_1, \omega) = n_0^{-1} \lim_{\gamma \rightarrow \infty} \left[\gamma^3 \overleftarrow{g} \overleftarrow{g} \overleftarrow{g} \text{---} - \gamma^4 \overleftarrow{g} \overleftarrow{g} \overleftarrow{g} \overleftarrow{g} \text{---} - \gamma^4 \overleftarrow{g} \overleftarrow{g} \overleftarrow{g} \overleftarrow{g} \text{---} - \gamma^4 \overleftarrow{g} \overleftarrow{g} \overleftarrow{g} \overleftarrow{g} \text{---} + \dots \right] \quad (\text{E16})$$

$$= n_0^{-1} \lim_{\gamma \rightarrow \infty} \left[\gamma^3 \overleftarrow{g} \sum_{r=0}^{\infty} (\gamma \overleftarrow{g})^r \times \overleftarrow{g} \times \sum_{s=0}^{\infty} (\gamma \overleftarrow{g})^s \times \overleftarrow{g} \times \sum_{t=0}^{\infty} (\gamma \overleftarrow{g})^t \times \text{---} \right] \quad (\text{E17})$$

$$= n_0^{-1} \lim_{\gamma \rightarrow \infty} \left[\gamma^3 \frac{1}{-i\omega} \frac{-\lambda\gamma}{1 + \gamma\kappa R(x_1, \omega)} \times \overleftarrow{g} \times \sum_{s=0}^{\infty} (\gamma \overleftarrow{g})^s \times \overleftarrow{g} \times \frac{\sigma\gamma}{1 + \gamma\kappa R(x_1, \omega)} T(x_0, x_1, \omega) \right] \quad (\text{E18})$$

Here, we made use again of the geometric sums in Eq. (D18) as well as Eqs. (E12)–(E14), which features three times in Eq. (E17), once with dummy index r , once with s and once with t . The central one, running with index s differs from the others by the (blue) dashed line that represents the noise carrying momentum $\tilde{\omega}$ thus bypassing the loops, so that only $\omega - \tilde{\omega}$ flows through loops summed over. Using Eq. (E14) in this loop, the effective vertex of $\mathcal{Q}_{II}^{(1)}(x_0, x_1, \omega)$ is

$$(x_1, \omega) \begin{array}{c} \tilde{\omega} \\ \partial_{y_2} \\ \text{---} \\ \partial_{y_1} \\ \omega - \tilde{\omega} \end{array} (x_1, \omega) \times \sum_{s=0}^{\infty} (\gamma \overleftarrow{g})^s \times \overleftarrow{g} \quad (\text{E19})$$

$$= \iint dy_1 dy_2 d\tilde{\omega} (\partial_{y_1} T(x_1, y_1, \omega)) T(y_1, x_1, \omega - \tilde{\omega}) \frac{1}{R(x_1, \omega - \tilde{\omega})} (\partial_{y_2} T(x_1, y_2, \omega - \tilde{\omega})) T(y_2, x_1, \omega) C_2(\tilde{\omega}), \quad (\text{E20})$$

to be contrasted with Eq. (E15), the effective vertex of $\mathcal{Q}_I^{(1)}(x_0, x_1, \omega)$.

Inserting the result (E20) into Eq. (E18), and using $n_0 = \sigma/\kappa$, we obtain an explicit formula

$$\mathcal{Q}_{II}^{(1)}(x_0, x_1, \omega) = \frac{1}{-i\omega} \frac{T(x_0, x_1)}{(R(x_1, \omega))^2} \iint dy_1 dy_2 d\tilde{\omega} \frac{(\partial_{y_1} T(x_1, y_1, \omega)) T(y_1, x_1, \omega - \tilde{\omega})}{R(x_1, \omega - \tilde{\omega})} (\partial_{y_2} T(x_1, y_2, \omega - \tilde{\omega})) T(y_2, x_1, \omega) C_2(\tilde{\omega}) \quad (\text{E21})$$

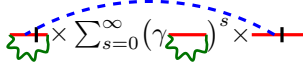
Thirdly, we consider $\mathcal{Q}_{III}^{(1)}$, shown as III) in Fig. 1, the case of the transition propagator, --- , coupling to one of the return propagators, \overleftarrow{g} , via $C_2(\omega)$ which results in the diagrammatic expansion

$$\mathcal{Q}_{III}^{(1)}(x_0, x_1, \omega) = n_0^{-1} \lim_{\gamma \rightarrow \infty} \left[-\gamma^2 \overleftarrow{g} \overleftarrow{g} \text{---} + \gamma^3 \overleftarrow{g} \overleftarrow{g} \overleftarrow{g} \text{---} + \gamma^3 \overleftarrow{g} \overleftarrow{g} \overleftarrow{g} \text{---} + \dots \right] \quad (\text{E22})$$

$$= n_0^{-1} \lim_{\gamma \rightarrow \infty} \left[\gamma^3 \overleftarrow{g} \sum_{r=0}^{\infty} (\gamma \overleftarrow{g})^r \times \overleftarrow{g} \times \sum_{s=0}^{\infty} (\gamma \overleftarrow{g})^s \times \text{---} \right] \quad (\text{E23})$$

$$= n_0^{-1} \lim_{\gamma \rightarrow \infty} \left[\gamma^3 \frac{1}{-i\omega} \frac{(-\lambda)\gamma}{1 + \gamma\kappa R(x_1, \omega)} \times \overleftarrow{g} \times \sum_{s=0}^{\infty} (\gamma \overleftarrow{g})^s \times \text{---} \right] \quad (\text{E24})$$

where we made use of the renormalisation of λ , Eq. (E12). For the remaining diagram in Eq. (E24), which differs from Eq. (E20) only by an incoming transition propagator instead of a return propagator, we find



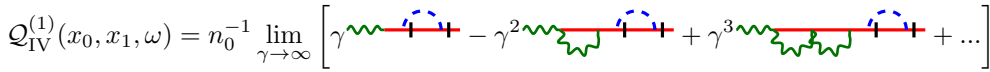
$$\times \sum_{s=0}^{\infty} (\gamma \text{ [red line with green wavy line] })^s \times \text{[red line with green wavy line]} \quad (\text{E25})$$

$$= \iint dy_1 dy_2 d\tilde{\omega} (\partial_{y_1} T(x_0, y_1, \omega)) T(y_1, x_1, \omega - \tilde{\omega}) \frac{\gamma(-\kappa)}{1 + \gamma\kappa R(x_1, \omega - \tilde{\omega})} (\partial_{y_2} T(x_1, y_2, \omega - \tilde{\omega})) T(y_2, x_1, \omega) C_2(\tilde{\omega}) \quad (\text{E26})$$

Inserting the result of Eq. (E26) into Eq. (E24), one obtains

$$\mathcal{Q}_{\text{III}}^{(1)}(x_0, x_1, \omega) = -\frac{1}{-i\omega} \frac{1}{R(x_1, \omega)} \iint dy_1 dy_2 d\tilde{\omega} \frac{(\partial_{y_1} T(x_0, y_1, \omega)) T(y_1, x_1, \omega - \tilde{\omega})}{R(x_1, \omega - \tilde{\omega})} (\partial_{y_2} T(x_1, y_2, \omega - \tilde{\omega})) T(y_2, x_1, \omega) C_2(\tilde{\omega}) \quad (\text{E27})$$

Finally, we consider $\mathcal{Q}_{\text{IV}}^{(1)}$, shown as IV) in Fig. 1, where two g -vertices couple into the incoming transition propagator,



$$\mathcal{Q}_{\text{IV}}^{(1)}(x_0, x_1, \omega) = n_0^{-1} \lim_{\gamma \rightarrow \infty} \left[\gamma \text{ [red line with green wavy line] } - \gamma^2 \text{ [red line with green wavy line] } + \gamma^3 \text{ [red line with green wavy line] } + \dots \right] \quad (\text{E28})$$

$$= n_0^{-1} \lim_{\gamma \rightarrow \infty} \left[\gamma \sum_{r=0}^{\infty} (\gamma \text{ [red line with green wavy line] })^r \text{ [red line with green wavy line] } \right] \quad (\text{E29})$$

$$= n_0^{-1} \lim_{\gamma \rightarrow \infty} \left[\gamma \frac{1}{-i\omega} \frac{(-\lambda)\gamma}{1 + \gamma\kappa R(x_1, \omega)} \right] \quad (\text{E30})$$

$$\times \iint dy_1 dy_2 d\tilde{\omega} (\partial_{y_1} T(x_0, y_1, \omega)) (\partial_{y_2} T(y_1, y_2, \omega - \tilde{\omega})) T(y_2, x_1, \omega) C_2(\tilde{\omega}) \quad (\text{E31})$$

$$= \frac{1}{-i\omega} \frac{1}{R(x_1, \omega)} \iint dy_1 dy_2 d\tilde{\omega} (\partial_{y_1} T(x_0, y_1, \omega)) (\partial_{y_2} T(y_1, y_2, \omega - \tilde{\omega})) T(y_2, x_1, \omega) C_2(\tilde{\omega}) \quad (\text{E32})$$

The trace function corrected to leading order in the external noise is thus given by

$$\mathcal{Q}(x_0, x_1, \omega) = \frac{T(x_0, x_1, \omega)}{(-i\omega)R(x_1, \omega)} + g^2 \left[\mathcal{Q}_{\text{I}}^{(1)} + \mathcal{Q}_{\text{II}}^{(1)} + \mathcal{Q}_{\text{III}}^{(1)} + \mathcal{Q}_{\text{IV}}^{(1)} \right] + \mathcal{O}(g^3) \quad (\text{E33})$$

Comparing the four correction terms, $\mathcal{Q}_{\text{I}}^{(1)}, \dots, \mathcal{Q}_{\text{IV}}^{(1)}$, it turns out that they draw on two different integrals,

$$\mathcal{J}_1(x_0, x_1, \omega) = \iint dy_1 dy_2 d\tilde{\omega} (\partial_{y_1} T(x_0, y_1, \omega)) (\partial_{y_2} T(y_1, y_2, \omega - \tilde{\omega})) T(y_2, x_1, \omega) C_2(\tilde{\omega}) \quad (\text{E34})$$

$$\mathcal{J}_2(x_0, x_1, \omega) = \iint dy_1 dy_2 d\tilde{\omega} \frac{(\partial_{y_1} T(x_0, y_1, \omega)) T(y_1, x_1, \omega - \tilde{\omega})}{R(x_1, \omega - \tilde{\omega})} (\partial_{y_2} T(x_1, y_2, \omega - \tilde{\omega})) T(y_2, x_1, \omega) C_2(\tilde{\omega}) \quad (\text{E35})$$

with \mathcal{J}_1 entering into $\mathcal{Q}_{\text{I}}^{(1)}$ and $\mathcal{Q}_{\text{IV}}^{(1)}$, Eqs. (E11) and (E32), and \mathcal{J}_2 entering into $\mathcal{Q}_{\text{II}}^{(1)}$ and $\mathcal{Q}_{\text{III}}^{(1)}$, Eqs. (E21) and (E27),

$$\mathcal{Q}_{\text{I}}^{(1)}(x_0, x_1, \omega) = -\frac{1}{-i\omega} \frac{T(x_0, x_1, \omega)}{(R(x_1, \omega))^2} \mathcal{J}_1(x_1, x_1, \omega) \quad (\text{E36})$$

$$\mathcal{Q}_{\text{II}}^{(1)}(x_0, x_1, \omega) = \frac{1}{-i\omega} \frac{T(x_0, x_1, \omega)}{(R(x_1, \omega))^2} \mathcal{J}_2(x_1, x_1, \omega) \quad (\text{E37})$$

$$\mathcal{Q}_{\text{III}}^{(1)}(x_0, x_1, \omega) = -\frac{1}{-i\omega} \frac{1}{R(x_1, \omega)} \mathcal{J}_2(x_0, x_1, \omega) \quad (\text{E38})$$

$$\mathcal{Q}_{\text{IV}}^{(1)}(x_0, x_1, \omega) = \frac{1}{-i\omega} \frac{1}{R(x_1, \omega)} \mathcal{J}_1(x_0, x_1, \omega). \quad (\text{E39})$$

Eq. (E33) simplifies further when factorising out the term to order g^0 :

$$\mathcal{Q}(x_0, x_1, \omega) = \frac{T(x_0, x_1, \omega)}{(-i\omega)R(x_1, \omega)} \left[1 + g^2 \left(\frac{\mathcal{J}_1(x_0, x_1, \omega) - \mathcal{J}_2(x_0, x_1, \omega)}{T(x_0, x_1, \omega)} - \frac{\mathcal{J}_1(x_1, x_1, \omega) - \mathcal{J}_2(x_1, x_1, \omega)}{R(x_1, \omega)} \right) \right] + \mathcal{O}(g^3) \quad (\text{E40})$$

To simplify notation, we introduce

$$T^{(2)}(x_0, x_1, \omega) = \mathcal{J}_1(x_0, x_1, \omega) - \mathcal{J}_2(x_0, x_1, \omega) \quad (\text{E41})$$

$$= \iint dy_1 dy_2 d\tilde{\omega} \left[(\partial_{y_2} T(y_1, y_2, \omega - \tilde{\omega})) - \frac{T(y_1, x_1, \omega - \tilde{\omega})}{R(x_1, \omega - \tilde{\omega})} (\partial_{y_2} T(x_1, y_2, \omega - \tilde{\omega})) \right] \times (\partial_{y_1} T(x_0, y_1, \omega)) T(y_2, x_1, \omega) C_2(\tilde{\omega}) \quad (\text{E42})$$

$$= \iint dy_1 dy_2 (\partial_{y_1} T(x_0, y_1, \omega)) (\partial_{y_2} T(y_2, x_1, \omega)) \times \int d\tilde{\omega} \left[\frac{T(y_1, x_1, \omega - \tilde{\omega})}{R(x_1, \omega - \tilde{\omega})} T(x_1, y_2, \omega - \tilde{\omega}) - T(y_1, y_2, \omega - \tilde{\omega}) \right] C_2(\tilde{\omega}) \quad (\text{E43})$$

where the last equality follows by integration by parts and re-arranging terms, arriving at Eq. (25). Using $T^{(2)}(x_0, x_1, \omega)$ in Eq. (E40) it may be written as

$$\mathcal{Q}(x_0, x_1, \omega) = \frac{T(x_0, x_1, \omega) + g^2 T^{(2)}(x_0, x_1, \omega)}{(-i\omega)(R(x_1, \omega) + g^2 T^{(2)}(x_1, x_1, \omega))} + \mathcal{O}(g^3). \quad (\text{E44})$$

In keeping with the notation of $T^{(2)}$ as the g^2 -correction to the transition probability, we henceforth write $T^{(0)}$ for what used to be called T , the contribution at $g = 0$. Collecting these terms into the *renormalised* T , we write

$$T(x_0, x_1, \omega) = T^{(0)}(x_0, x_1, \omega) + g^2 T^{(2)}(x_0, x_1, \omega) + \mathcal{O}(g^3) \quad (\text{E45})$$

and along the same lines the return probability

$$R(x_1, \omega) = T(x_1, x_1, \omega) = R^{(0)}(x_1, \omega) + g^2 R^{(2)}(x_1, \omega) + \mathcal{O}(g^3) = T^{(0)}(x_1, x_1, \omega) + g^2 T^{(2)}(x_1, x_1, \omega) + \mathcal{O}(g^3), \quad (\text{E46})$$

so that

$$\mathcal{Q}(x_0, x_1, \omega) = \frac{T(x_0, x_1, \omega)}{(-i\omega)R(x_1, \omega)} + \mathcal{O}(g^3). \quad (\text{E47})$$

Appendix F: Derivation of effective transition probability for Brownian Motion driven by self-correlated noise

To compute $T^{(2)}(x, \omega)$ in Eq. (E43), we firstly express the Fourier-transformed correlation function $\hat{C}_2(\omega)$ in terms of the inverse Laplace transform $\bar{C}_2(\beta)$, using

$$\hat{C}_2(\omega) = \int_{-\infty}^{\infty} dt e^{-i\omega t} C(|t|) = \int_{-\infty}^{\infty} dt e^{-i\omega t} \int_0^{\infty} d\beta e^{-\beta|t|} \bar{C}_2(\beta) \quad (\text{F1})$$

$$= 2 \int_0^{\infty} d\beta \left(\int_0^{\infty} dt \cos(\omega t) e^{-\beta t} \right) \bar{C}_2(\beta) \quad (\text{F2})$$

$$= \int_0^{\infty} d\beta \frac{2\beta}{\omega^2 + \beta^2} \bar{C}_2(\beta), \quad (\text{F3})$$

which facilitates the calculation of the convolution over $\tilde{\omega}$ in the second line of Eq. (E43), in particular when we consider exponential correlations, Eq. (31), in which case $\bar{C}_2(\beta) \propto \delta(\beta - \beta^*)$. We first consider the convolution of C_2 with $T^{(0)}$,

$$\int d\tilde{\omega} T^{(0)}(y_1, y_2, \omega - \tilde{\omega}) C_2(\omega) = \int_0^{\infty} d\beta \int d\tilde{\omega} T^{(0)}(y_1, y_2, \omega - \tilde{\omega}) \frac{2\beta \bar{C}_2(\beta)}{\tilde{\omega}^2 + \beta^2} \quad (\text{F4})$$

$$= \int_0^{\infty} d\beta \bar{C}_2(\beta) T^{(0)}(y_1, y_2, \omega + i\beta), \quad (\text{F5})$$

where we have used that $T^{(0)}(y_1, y_2, \omega)$ cannot have any poles in the upper half-plane, because its inverse Fourier transform $T^{(0)}(y_1, y_2, \tau)$ must vanish for all $\tau < 0$. If there were any poles in the upper half-plane, the auxiliary path that for $\tau < 0$ must pass through the upper half plane would enclose them, producing $T^{(0)}(y_1, y_2, \tau) \neq 0$.

Considering secondly the convolution of C_2 with the term of the form $T^{(0)}T^{(0)}/R^{(0)}$ in Eq. (E43), we similarly obtain

$$\int d\tilde{\omega} \frac{T^{(0)}(y_1, x_1, \omega - \tilde{\omega})}{R^{(0)}(x_1, \omega - \tilde{\omega})} T^{(0)}(x_1, y_2, \omega - \tilde{\omega}) C_2(\tilde{\omega}) = \int d\tilde{\omega} \chi_{\text{FPT}}^{(0)}(y_1, x_1, \omega - \tilde{\omega}) T^{(0)}(x_1, y_2, \omega - \tilde{\omega}) \int_0^\infty d\beta \frac{2\beta \bar{C}_2(\beta)}{\tilde{\omega}^2 + \beta^2} \quad (\text{F6})$$

$$= \int_0^\infty d\beta \bar{C}_2(\beta) \chi_{\text{FPT}}^{(0)}(y_1, x_1, \omega + i\beta) T^{(0)}(x_1, y_2, \omega + i\beta) = \int_0^\infty d\beta \bar{C}_2(\beta) \frac{T^{(0)}(y_1, x_1, \omega + i\beta)}{R^{(0)}(x_1, \omega + i\beta)} T^{(0)}(x_1, y_2, \omega + i\beta) \quad (\text{F7})$$

where we made use of the Markovian formula, Eqs. (B22) and (5), $\chi_{\text{FPT}}^{(0)}(\omega) = T^{(0)}(x_0, x_1; \omega)/R^{(0)}(x_1; \omega)$, which is, like $T^{(0)}(y_1, y_2, \omega)$ above, a Fourier transform of a probability density that vanishes for all $\tau < 0$ and thus has no poles in the upper half-plane.

Having performed the convolutions over $\tilde{\omega}$, turning them into easier integrals over β , what remains are the two spatial integrals over y_1 and y_2 ,

$$T^{(2)}(x_0, x_1, \omega) = \int_0^\infty d\beta \bar{C}_2(\beta) \iint dy_1 dy_2 \left[\frac{T^{(0)}(y_1, x_1, \omega + i\beta)}{R^{(0)}(x_1, \omega + i\beta)} T^{(0)}(x_1, y_2, \omega + i\beta) - T^{(0)}(y_1, y_2, \omega + i\beta) \right] \times \left(\partial_{y_1} T^{(0)}(x_0, y_1, \omega) \right) \left(\partial_{y_2} T^{(0)}(y_2, x_1, \omega) \right) \quad (\text{F8})$$

We proceed by calculating $T^{(2)}(x_0, x_1, \omega)$ for the particular case of Brownian Motion, which has transition propagator

$$T^{(0)}(x_0, x_1, \omega) = \int d\mathbf{k} \frac{e^{i\mathbf{k}(x_1-x_0)}}{-i\omega + D_x k^2} = \frac{e^{-|x_1-x_0|\sqrt{-\frac{i\omega}{D_x}}}}{\sqrt{-4i\omega D_x}}. \quad (\text{F9})$$

Beginning with the simpler integrand in Eq. (F8), the first term we consider is

$$\mathcal{I}_1(x_0, x_1, \omega) = \int_0^\infty d\beta \bar{C}_2(\beta) \iint dy_1 dy_2 T^{(0)}(y_1, y_2, \omega + i\beta) \left(\partial_{y_1} T^{(0)}(x_0, y_1, \omega) \right) \left(\partial_{y_2} T^{(0)}(y_2, x_1, \omega) \right) \quad (\text{F10})$$

$$= \int_0^\infty d\beta \bar{C}_2(\beta) \iint dy_1 dy_2 \iint dk dp dq \frac{e^{i\mathbf{k}(y_2-y_1)}}{-i\omega + D_x k^2 + \beta} \frac{(ip)e^{ip(y_1-x_0)}}{-i\omega + D_x p^2} \frac{(-iq)e^{iq(x_1-y_1)}}{-i\omega + D_x q^2} \quad (\text{F11})$$

Integration over both y_1 and y_2 results in two delta functions $\delta(k-p)$ and $\delta(p-q)$, respectively. Integrating over both $d\mathbf{k}$ and $d\mathbf{q}$ then results in

$$\mathcal{I}_1(x_0, x_1, \omega) = \int_0^\infty d\beta \bar{C}_2(\beta) \int d\mathbf{p} \frac{p^2 e^{ip(x_1-x_0)}}{(-i\omega + D_x p^2)^2 (-i\omega + D_x p^2 + \beta)}, \quad (\text{F12})$$

which using partial fractions can be expressed in terms of the Markovian transition densities (*cf* [26, Eq. (125)]),

$$\mathcal{I}_1(x_0, x_1, \omega) = \int_0^\infty d\beta \bar{C}_2(\beta) \int d\mathbf{p} \left(\frac{1}{\beta} \frac{p^2 e^{ip(x_1-x_0)}}{(-i\omega + D_x p^2)^2} - \frac{1}{\beta^2} \frac{p^2 e^{ip(x_1-x_0)}}{-i\omega + D_x p^2} + \frac{1}{\beta^2} \frac{p^2 e^{ip(x_1-x_0)}}{-i\omega + D_x p^2 + \beta} \right) \quad (\text{F13})$$

$$= - \int_0^\infty d\beta \bar{C}_2(\beta) \beta^{-2} (\partial_{x_1}^2) \left[-i\partial_\omega \beta T^{(0)}(x_0, x_1, \omega) - T^{(0)}(x_0, x_1, \omega) + T^{(0)}(x_0, x_1, \omega + i\beta) \right]. \quad (\text{F14})$$

Expressing $T^{(0)}(x_0, x_1, \omega)$ as a Fourier-transform in t , further leads to

$$\mathcal{I}_1(x_0, x_1, \omega) = - \int_0^\infty d\beta \bar{C}_2(\beta) \int dt e^{i\omega t} \beta^{-2} [\beta t - 1 + e^{-\beta t}] (\partial_{x_1}^2) T^{(0)}(x_0, x_1, t) \quad (\text{F15})$$

$$= - \int_0^\infty d\beta \bar{C}_2(\beta) \int dt e^{i\omega t} t^2 Y(\beta t) (\partial_{x_1}^2) T^{(0)}(x_0, x_1, t) \quad (\text{F16})$$

where we introduced the dimensionless scaling function

$$Y(z) = \frac{e^{-z} - 1 + z}{z^2} \quad (\text{F17})$$

with $Y(z) \xrightarrow{z \rightarrow 0} 1/2$ and $Y(z) \xrightarrow{z \gg 1} z^{-1}$. While $Y(z)$ is specific to Brownian Motion, other stochastic processes give rise to similar scaling functions as [26, Eq. (97)] indicates for the case of an Ornstein-Uhlenbeck process.

The second contribution of Eq. (F8) is

$$\mathcal{I}_2(x_0, x_1, \omega) \quad (\text{F18})$$

$$= \int_0^\infty d\beta \bar{C}_2(\beta) \iint dy_1 dy_2 \frac{T^{(0)}(y_1, x_1, \omega + i\beta)}{R^{(0)}(x_1, \omega + i\beta)} T^{(0)}(x_1, y_2, \omega + i\beta) (\partial_{y_1} T(x_0, y_1, \omega)) (\partial_{y_2} T^{(0)}(y_2, x_1, \omega)) \quad (\text{F19})$$

$$= \int_0^\infty d\beta \bar{C}_2(\beta) \sqrt{4D_x(\beta - i\omega)} \iint dy_1 dy_2 \iint dk_1 dk_2 dp dq \quad (\text{F20})$$

$$\frac{e^{ik_1(x_1 - y_1)}}{-i\omega + D_x k_1^2 + \beta} \frac{e^{ik_2(y_2 - x_1)}}{-i\omega + D_x k_2^2 + \beta} \frac{(ip)e^{ip(y_1 - x_0)}}{-i\omega + D_x p^2} \frac{(-iq)e^{iq(x_1 - y_2)}}{-i\omega + D_x q^2} ,$$

using $1/R^{(0)}(x_1, \omega + i\beta) = 1/T^{(0)}(x_1, x_1, \omega + i\beta) = \sqrt{4D_x(\beta - i\omega)}$, Eq. (F9). Integrating over y_1 and y_2 produces two δ -functions, $\delta(p - k_1)\delta(q - k_2)$. Using them when integrating over k_1, k_2 gives

$$\mathcal{I}_2(x_0, x_1, \omega) = \int_0^\infty d\beta \bar{C}_2(\beta) \sqrt{4D_x(\beta - i\omega)} \quad (\text{F21})$$

$$\times \left(\int dq \frac{(-iq)}{(-i\omega + D_x q^2)(-i\omega + D_x q^2 + \beta)} \right) \left(\int dp \frac{(ip)e^{ip(x_1 - x_0)}}{(-i\omega + D_x p^2)(-i\omega + D_x p^2 + \beta)} \right)$$

By symmetry, the integral over dq vanishes and thus $\mathcal{I}_2 = 0$. For Brownian Motion, we thus obtain for $T^{(2)}(x_0, x_1, \omega)$, Eqs. (25) and (E43),

$$T^{(2)}(x_0, x_1, \omega) = -\mathcal{I}_1(x_0, x_1, \omega) = \int_0^\infty d\beta \bar{C}_2(\beta) \int dt e^{i\omega t} t^2 Y(\beta t) (\partial_{x_1}^2) T^{(0)}(x_0, x_1, t) \quad (\text{F22})$$

By inverting the Fourier transform we further obtain

$$T^{(2)}(x_0, x_1, t) = \int_0^\infty d\beta \bar{C}_2(\beta) t^2 Y(\beta t) (\partial_{x_1}^2) T^{(0)}(x_0, x_1, t) \quad (\text{F23})$$

$$= \Upsilon(t) (\partial_{x_1}^2) T^{(0)}(x_0, x_1, t) \quad (\text{F24})$$

where we introduced the time-stretch function, Eq. (27),

$$\Upsilon(t) = \int_0^\infty d\beta \bar{C}_2(\beta) t^2 Y(\beta t) \quad (\text{F25})$$

$$= \int_0^\infty d\beta \frac{\bar{C}_2(\beta)}{\beta^2} [e^{-\beta t} - 1 + \beta t] . \quad (\text{F26})$$

Making use of the properties of the Laplace transform, we find

$$\int_0^\infty d\beta \beta^{-2} e^{-\beta t} \bar{C}_2(\beta) = \int_0^\infty ds s C_2(t + s) \quad (\text{F27})$$

$$\int_0^\infty d\beta \beta^{-2} \bar{C}_2(\beta) = \int_0^\infty ds s C_2(s) \quad (\text{F28})$$

$$\int_0^\infty d\beta \beta^{-1} t \bar{C}_2(\beta) = \int_0^\infty ds t C_2(s) \quad (\text{F29})$$

and after some simple transformations,

$$\Upsilon(t) = \int_0^\infty ds (s C_2(t + s) - s C_2(s) + t C_2(s)) = \int_0^t ds (t - s) C_2(s) = \int_0^t ds \int_0^s du C_2(u) , \quad (\text{F30})$$

as in Eq. (27).

Appendix G: List of explicit results for visit probabilities

The concrete perturbative corrections resulting from formulas (24) and (25) are often cumbersome expressions. The correction for the active thermal Brownian Motion on a real line, characterised by (26), and with an exponentially correlated driving noise is given implicitly via Eq. (30). This integral can be performed using Mathematica [44] and delivers

$$\mathcal{Q}(x, \omega) = \frac{e^{-\sqrt{\frac{-i\omega x^2}{D_x}}}}{-i\omega} \left[1 + \frac{g^2 D_y}{D_x^2 \beta} \left(D_x \sqrt{(-i\omega)(\beta - i\omega)} \left(e^{-\frac{\sqrt{\beta - i\omega} - \sqrt{-i\omega}}{\sqrt{D_x}} |x|} - 1 \right) + \frac{1}{2} \beta \sqrt{-i D_x \omega} |x| \right) \right] \quad (\text{G1})$$

In the joint limit of $\beta \rightarrow 0$ and $D_y \beta = w^2$ fixed, the moment generating function becomes

$$\mathcal{Q}(x, \omega) = \frac{e^{-\sqrt{\frac{-i\omega x^2}{D_x}}}}{-i\omega} \left[1 + \frac{g^2 w^2}{8 D_x^2} \left(x^2 - \sqrt{\frac{D_x x^2}{-i\omega}} \right) \right] \quad (\text{G2})$$

This corresponds to the visit probability of a Brownian motion with a random but fixed additional drift term y which is Gaussian distributed with mean zero and variance w^2 .

In [26], we developed a perturbative framework which was able to compute the moment-generating functions of first-passage time distributions for processes of the form (17). This framework did not use field theory, but instead a functional perturbation theory. Since $\mathcal{Q}(x, \omega) = \frac{1}{-i\omega} \chi_{\text{FPT}}(x, \omega)$, we here report the findings for two other models first reported there, for future reference.

First, we report the visit probability of an active Brownian Motion on a ring of radius r , hence

$$\dot{x}_t = \xi_t + g y_t \quad x_t \equiv x_t + 2\pi r. \quad (\text{G3})$$

We then study the visit probability over a certain angle $\theta = \frac{x_1 - x_0}{r}$. As a shorthand, we further introduce the inverse diffusive timescale $\alpha^{-1} = r^2/D_x$. To leading perturbative order, the visit probability is then given by [26, Eq. (127)]

$$\begin{aligned} \mathcal{Q}(\theta, \omega) &= \frac{\cosh((\theta - \pi)\sqrt{-i\alpha^{-1}\omega})}{(-i\omega) \cosh(\pi\sqrt{-i\alpha^{-1}\omega})} \\ &+ \frac{D_y g^2}{2D_x} \cdot \frac{\sqrt{-i\alpha^{-1}\omega} \tanh(\pi\sqrt{-i\alpha^{-1}\omega})}{-i\alpha^{-1}\beta\omega} \left[\frac{\cosh((\theta - \pi)\sqrt{\alpha^{-1}(\beta - i\omega)})}{\sinh(\pi\sqrt{\alpha^{-1}(\beta - i\omega)})} 2\sqrt{\alpha^{-1}(\beta - i\omega)} \right. \\ &\left. + \frac{\cosh((\theta - \pi)\sqrt{-i\alpha^{-1}\omega})}{\cosh(\pi\sqrt{-i\alpha^{-1}\omega})} \left(\pi\bar{\beta} - 2\sqrt{\alpha^{-1}(\beta - i\omega)} \coth(\pi\sqrt{\alpha^{-1}(\beta - i\omega)}) \right) + \frac{\sinh((\theta - \pi)\sqrt{-i\alpha^{-1}\omega})}{\sinh(\pi\sqrt{-i\alpha^{-1}\omega})} \bar{\beta}(\pi - \theta) \right] \end{aligned} \quad (\text{G4})$$

$$(\text{G5})$$

In the limit of infinite radius, $r \rightarrow \infty$, one finds $\theta\sqrt{-i\alpha^{-1}\omega} \rightarrow \sqrt{-i\frac{\omega(x_1 - x_0)^2}{D_x}}$, and accordingly the Markovian result converges, as expected to

$$\lim_{r \rightarrow \infty} \frac{\cosh((\theta - \pi)\sqrt{-i\alpha^{-1}\omega})}{(-i\omega) \cosh(\pi\sqrt{-i\alpha^{-1}\omega})} = \lim_{r \rightarrow \infty} \frac{1}{(-i\omega)} \frac{\cosh\left(\sqrt{-i\frac{\omega}{D_x}} |x_1 - x_0| - \sqrt{-i\frac{\omega}{D_x}} \pi r\right)}{\cosh\left(\sqrt{-i\frac{\omega}{D_x}} \pi r\right)} = \frac{e^{\sqrt{-i\frac{\omega}{D_x}} |x_1 - x_0|}}{-i\omega} \quad (\text{G6})$$

Analogously, a more involved computation using, for instance, Mathematica confirms that

$$\lim_{r \rightarrow \infty} \mathcal{Q}^{\text{ring}}\left(\frac{x_1 - x_0}{r}, \omega\right) = \mathcal{Q}^{\text{line}}(x_1 - x_0, \omega) \quad (\text{G7})$$

with $\mathcal{Q}^{\text{ring}}(\frac{x_1 - x_0}{r}, \omega)$ being the result in Eq. (G4) and $\mathcal{Q}^{\text{line}}(x_1 - x_0, \omega)$ the perturbative result found in Eq. (G1).

Finally we consider the case of a harmonic trap, ie.

$$\dot{x}_t = -\alpha x + \xi_t + g y_t. \quad (\text{G8})$$

which we refer to as active thermal Ornstein Uhlenbeck process (ATOU). The result is more compactly given in dimensionless units

$$\bar{\beta} = \alpha^{-1}\beta \quad \bar{x}_0 = x_0/\ell \quad \bar{x}_1 = x_1/\ell \quad \text{with} \quad \ell = \sqrt{D_x \alpha^{-1}} \quad (\text{G9})$$

The Fourier transformed visit probability is given in terms of parabolic cylinder functions $D_{-\nu}(x)$ ([45]) and reads (for $x_0 < x_1$) [26, Eq. (100)]

$$\mathcal{Q}(x, \omega) = e^{\frac{x_0^2 - x_1^2}{4}} \frac{D_{i\alpha^{-1}\omega}(\bar{x}_0)}{(-i\omega)D_{i\alpha^{-1}\omega}(\bar{x}_1)} \quad (\text{G10})$$

$$\begin{aligned} &+ \frac{g^2 D_y \bar{\beta}}{D_x (-i\omega)} \frac{(-i\alpha^{-1}\omega) e^{\frac{x_0^2 - x_1^2}{4}}}{2(\bar{\beta}^2 - 1) D_{i\alpha^{-1}\omega}(-\bar{x}_1)^2 D_{-\bar{\beta} + i\alpha^{-1}\omega}(-\bar{x}_1)} \\ &\times [(\bar{\beta} + 1)(-i\alpha^{-1}\omega + 1) D_{-\bar{\beta} + i\alpha^{-1}\omega}(-\bar{x}_1) (D_{i\alpha^{-1}\omega}(-\bar{x}_0) D_{i\alpha^{-1}\omega - 2}(-\bar{x}_1) - D_{i\alpha^{-1}\omega - 2}(-\bar{x}_0) D_{i\alpha^{-1}\omega}(-\bar{x}_1)) \\ &\quad - 2(\bar{\beta} - i\alpha^{-1}\omega) D_{i\alpha^{-1}\omega - 1}(-\bar{x}_1) (D_{i\alpha^{-1}\omega}(-\bar{x}_0) D_{-\bar{\beta} + i\alpha^{-1}\omega - 1}(-\bar{x}_1) - D_{-\bar{\beta} + i\alpha^{-1}\omega - 1}(-\bar{x}_0) D_{i\alpha^{-1}\omega}(-\bar{x}_1))] \end{aligned} \quad (\text{G11})$$
